

# Viabilidade e Eficiência dos Sistemas de Captura de Carbono: Análise e Alternativas para Mitigação das Emissões de CO<sub>2</sub>



## Relatório da Dissertação do M.EM

Orientadora no INEGI: Eng. Géssika Morgado

Orientador na FEUP: Prof. Abel Rouboa

João Miguel Araújo de La Puente Furtado ([up201806889@up.pt](mailto:up201806889@up.pt))

Porto, julho de 2024

# Resumo

O Painel Intergovernamental das alterações climáticas no seu relatório especial relativo ao aquecimento global referiu uma corrida urgente para atingir emissões líquidas nulas em carbono até ao meio do século por forma a prevenir consequências catastróficas. Todos os possíveis cenários para atingir estas emissões líquidas nulas de carbono dependem da adoção de planos de captura de  $CO_2$ .

Esta dissertação foi escrita com o intuito de estudar diferentes formas de mitigar as emissões provenientes de grandes emissores de carbono como é o caso de estações de incineração, fábricas de produção de vidro, cimenteiras e fábricas de produção de papel.

Foi realizada uma breve comparação entre as diferentes principais tecnologias de captura de carbono utilizadas atualmente bem como todos os aspetos associados à necessária compressão e transporte do  $CO_2$  desde a sua fonte até ao destino final.

Na secção relativa ao transporte do  $CO_2$ , foram exploradas todas as características associadas aos quatro principais meios de transportar o  $CO_2$ : barco, camião, comboio e transporte em tubagem.

Os resultados obtidos através deste estudo mostram que para o caso do transporte de 400 000 t $CO_2$ /ano provenientes das emissões de uma incineradora até a um porto de mar localizado a 6 km de distância, através de uma análise económica, concluiu-se que a dimensão para a tubagem mais eficaz economicamente corresponde a utilizar um diâmetro de 125 mm, com o  $CO_2$  a ser injetado a uma pressão de 105.85 bar resultando num custo total nivelado para o transporte do  $CO_2$  de 19.05 €/t (este valor engloba os custos associados ao investimento e operação + manutenção de toda a tubagem, compressor e bomba, bem como os custos energéticos associados ao compressor e à bomba).

Resultados chave deste estudo mostraram qual seria a dimensão mais adequada a escolher para a tubagem considerando caudais mássicos de  $CO_2$  a variar na gama de 200 000 a 800 000 t/ano e comprimentos de tubagem de 5 a 100 km, bem como a distância na tubagem onde seria mais apropriada a colocação de estações de repressurização dependendo do caudal de  $CO_2$  a transportar. Isto é informação crucial dado que a adição de uma estação de repressurização afeta drasticamente o custo do transporte do  $CO_2$ .

# Abstract

The Intergovernmental Panel on Climate Change (IPCC) in its special report on global warming refer to an urgent rush for achieving net-zero emissions by mid-century in order to prevent catastrophic consequences. And all possible scenarios for achieving this net-zero emissions depend on  $CO_2$  capture plans.

This dissertation was written with the goal of studying different ways of mitigating the emissions coming from big carbon dioxide sources such as waste incineration facilities, glass production factories, or cement and paper production factories.

It was done a brief comparison between the current main technologies for carbon capture. And all the aspects associated to the necessary compression and transport of  $CO_2$  from the source to the final destination were also analysed.

On the  $CO_2$  transport subsection it was depicted all the characteristics associated to the four main transportation methods that are: ship, truck, rail and pipeline transport.

The results obtained from this study show that for the case of transporting 400 000 t $CO_2$ /year from the emissions of a waste incineration facility into a seaport at a distance of 6 km, from an economical analysis approach, it was concluded that the most cost-beneficial size for the pipeline diameter should be 125 mm, the  $CO_2$  should be injected on the pipeline with a pressure of 105.85 bar resulting on a total levelized cost for  $CO_2$  transport (LCO<sub>2</sub>T) of 19.05 €/t (this value includes the costs associated to the pipe investments and operations and maintenance, the compressor and pump investment plus operations and maintenance and the compressor and pump energy consumption).

Key findings from this study shown what would be the most suitable pipe size to adopt considering a  $CO_2$  mass flow that range from 200 000 to 800 000 t/year and a pipeline length that range from 5 to 100 km, as well as the exact distance in the pipeline from where a booster station would need to be placed depending on the mass flow to be transported. This is a crucial information since the inclusion of a booster station drastically impacts the levelized cost of  $CO_2$  transport (LCO<sub>2</sub>T).

# Contents

<b>1</b>	<b>Introduction</b>	<b>1</b>
<b>2</b>	<b>Literature Review</b>	<b>2</b>
2.1	Climate Change . . . . .	2
2.1.1	Observed Changes and their Causes . . . . .	2
2.1.2	Adaptation and Mitigation . . . . .	4
2.1.3	Total Final Energy Consumption and Emissions by Sector . . . . .	4
2.1.4	National and EU goals for climate change mitigation . . . . .	5
2.2	Carbon Capture and Storage . . . . .	6
2.2.1	The need for CCS . . . . .	6
2.3	Technologies for Carbon capture . . . . .	8
2.3.1	Pre-combustion Capture . . . . .	10
2.3.2	Post-Combustion Capture . . . . .	12
2.3.3	Oxy-Combustion Capture . . . . .	19
2.4	The Transport Sector . . . . .	19
2.4.1	National and EU goals for the implementation of synthetic fuels on the transport sector . . . . .	21
<b>3</b>	<b>CO<sub>2</sub> Compression and Transport</b>	<b>22</b>
3.1	CO <sub>2</sub> Compression . . . . .	22
3.2	CO <sub>2</sub> transport . . . . .	28
3.2.1	Ship Transport . . . . .	29
3.2.2	Truck Transport . . . . .	29
3.2.3	Rail Transport . . . . .	30
3.2.4	Pipeline Transport . . . . .	31
3.2.5	Comparison of Characteristics for CO <sub>2</sub> Transport Methods . . . . .	35

3.3	Economics of $CO_2$ Compression and Transport . . . . .	37
3.3.1	Pipeline Costs . . . . .	37
3.3.2	Compressor and Pump Costs . . . . .	38
<b>4</b>	<b>Case Study</b>	<b>43</b>
4.1	Executive Summary . . . . .	43
4.2	Problem Set up and Assumptions . . . . .	43
4.3	Results And Discussion . . . . .	45
4.3.1	Cost Analysis Results . . . . .	49
<b>5</b>	<b>Conclusion</b>	<b>56</b>
<b>6</b>	<b>References</b>	<b>57</b>
	<b>Appendices</b>	<b>I</b>
A	Annex Physical properties of carbon dioxide . . . . .	I
B	Pipe size of seamless steel pipe DIN 2448 . . . . .	III

# List of Figures

1	Human-induced warming reached approximately 1°C above pre-industrial levels in 2017. At the present rate, global temperatures would reach 1.5°C around 2040. Stylized 1.5°C pathway shown here involves emission reductions beginning immediately, and CO2 emissions reaching zero by 2055, [6]. . . . .	3
2	Global CO2 emissions from energy combustion and industrial processes and their annual change, 1900-2022, [8]. . . . .	3
3	Global CO2 emissions by sector, 2019-2022, [8]. . . . .	4
4	CO2 CAPTURE CAPACITY IN 2020 AND 2050 BY FUEL AND SECTOR IN THE IEA SUSTAINABLE DEVELOPMENT SCENARIO, [3]. . . . .	7
5	TRL assessment and key technology vendors of the CO2 capture technologies, [10]. . . . .	9
6	TRL assessment and key technology vendors of the CO2 capture technologies, [10]. . . . .	10
7	Typical IGCC AGR Process Arrangement for CO2 Capture , [4]. . . . .	11
8	Chart for Selecting CO2 Removal Technologies Available Commercially , [9]. . . . .	12
9	Schematic of Amine-Based Post-Combustion CO2 Capture Process, [9]. . . . .	14
10	Relative Permeabilities of Gases in Polydimethylsiloxane, [9]. . . . .	16
11	Common Membrane Module Designs, [9]. . . . .	18
12	Energy demand in aviation by fuel and scenario, 2022-2050, and annual fuel intensity improvement rate, 2019-2050, [7]. . . . .	20
13	Comparison of Isentropic, Isothermal, and Intercooled Polytropic CO2 Compression ( $\eta_{pol} = 86\%$ ) Paths For compressing CO2 at 23.5 psia, 70°F (21°C) to 2215 psia., [9]. . . . .	25
14	Inlet and Outlet Pressures for CO2 Compression Using Conventional Centrifugal Compression with Intercooling Between Stages, [9]. . . . .	25
15	Schematic of Two-Stage Compression of CO2 Using Shock Wave Compression, [9]. . . . .	26
16	p-H Diagram for Conventional and High-Pressure Ratio CO2 Compression ( $\eta_p = 86\%$ ), [9]. . . . .	27
17	Stage Outlet Temperature, Head, and Overall Compression Load for the Two-Stage Compression of CO2 from 23.5–2,215 psia using Prode and Schultz calculations, [9]. . . . .	27
18	Example CO2 source and transportation options, [12]. . . . .	29
19	Transport truck for refrigerated liquid (left-side) and portable liquid CO2 storage container (right-side), [12]. . . . .	30

20	400 mm diameter commercial CO <sub>2</sub> pipeline at above/below ground transition, [12]. . . . .	32
21	CO <sub>2</sub> processing block diagram, [15]. . . . .	39
22	CO <sub>2</sub> phase diagram, [15]. . . . .	40
23	Pipeline Outline. . . . .	44
24	Flowsheet used on Aspen Plus. . . . .	45
25	Multi stage compressor profile results. . . . .	46
26	Multi stage compressor inter stage cooling results. . . . .	47
27	Summary of the simulation results attained for the pump part A. . . . .	47
28	Summary of the simulation results attained for the pump part B. . . . .	48
29	Levelized cost of carbon dioxide transport for different pipe diameters. . . . .	53
30	Sensitivity analysis for pipe DN 125 mm. . . . .	53
31	Least Levelized transport cost of CO <sub>2</sub> including initial compression for different mass flow rates. . . . .	54
32	Least Levelized transport cost of CO <sub>2</sub> including initial compression for different mass flow rate and distances considering pipe sizes of 100, 125, 150 and 200 mm. . . . .	55
33	Maximum safety distance for CO <sub>2</sub> pipeline transportation without a booster station. . . . .	55
A.1	A phase diagram for CO <sub>2</sub> ., adapted from [11]. . . . .	I
A.2	Nonlinear compressibility of CO <sub>2</sub> in the range of pressures common for pipeline transport as predicted by the Peng-Robinson equation of state, [11]. . . . .	II
B.1	Pipe size of seamless steel pipe DIN 2448. . . . .	III

## List of Tables

1	Simplified definitions of Technology Readiness Level (TRL) for CCS technologies, [10]. . . . .	8
2	Existing Pipeline Specifications, [12]. . . . .	34
3	Key characteristics for CO <sub>2</sub> transport methods, [12]. . . . .	36
4	Assumptions used for the simulation. . . . .	46
5	Assumptions used for the simulation. . . . .	48

6	Pipeline-related assumptions. . . . .	49
7	Pipeline-related cost results. . . . .	50
8	Compressor and pump-related assumptions. . . . .	50
9	Compressor -related assumptions. . . . .	51
10	Pump-related assumptions. . . . .	51
11	Compressor and pump-related cost results. . . . .	52

# Nomenclature

- $C_{0,comp}$  Base cost of the compressor at 2010 [M€]
- $C_{0,pump}$  Base cost of the pump [K€]
- $C_{comp}$  Cost of the compressor [M€]
- $C_{pump}$  Costs associated to the pump [K€]
- $C_{total}$  Total investment cost for the compressor and pump [€]
- $CF_{comp/pump}$  Capacity factor of the compressor and pump
- $CF_{pipe}$  Capital factor for pipeline
- $C_p$  Specific heat at constant pressure [ $J/kg * K$ ]
- $CRF$  Capital recovery factor
- $CRF_{comp/pump}$  Capital recovery factor for compressor and pump
- $CRF_{pipe}$  Capital recovery factor for pipeline
- $C_v$  Specific heat at constant volume [ $J/kg * K$ ]
- D Pipeline internal Diameter [m]
- DN Pipeline normalized diameter [m]
- E Longitudinal joint factor
- $E_{annual}$  Annual energy cost for compression and pumping [€]
- F Design factor
- f Darcy factor
- $H_p^{idealgas}$  Polytropic head for compressing an ideal gas [ $J/kg$ ]
- $H_p^{realgas}$  Polytropic head for compressing a real gas [ $J/kg$ ]
- $H_R^{idealgas}$  Actual (effective) head for compressing an ideal gas [ $J/kg$ ]
- $H_R^{realgas}$  Actual (effective) head for compressing a real gas [ $J/kg$ ]
- $I_{cum}$  Cumulative inflation rate of € from 2010 to 2024
- $IC_{pipe}$  Investment cost for the pipeline [€/m]
- $Invest_{pipe}$  Total investment cost of the pipeline [€]

$i$  Interest rate

$K_s$  Average ratio of specific heats of  $CO_2$  for each compression stage

$L$  Pipeline length [m]

$LCO2_{comp/pump,Energy}$  LCO2T for initial compressor and pump energy costs [€/t]

$LCO2T_{comp/pump,Invest}$  Least levelized cost for  $CO_2$  transportation for the initial compressor and pump investment [€/t]

$LCO2T_{pipe}$  Levelized cost of pipeline transport [€/t]

$LCO2T_{pipe,Invest}$  Levelized cost of carbon dioxide transport for pipeline investment [€/t]

$LCO2T_{pipe,O\&M}$  Levelized cost of pipeline O&M [€/t]

$M$  Molecular weight of  $CO_2$  [kg/Kmol]

$MolWt$  Molecular Weight [kg/mol]

$m$  Mass flow rate of  $CO_2$  [t/day]

$m_{CO_2,year}$  Amount of CO2 transported in a year [t/year]

$me$  Multiplication exponent

$N_{train,comp}$  Number of parallel compressor units

$N_{train,pump}$  Number of parallel pump units

$n$  Lifetime years

$n_{pol}$  Polytropic exponent

$O\&M_{annual}$  Annual operation and maintenance cost of compressor and pump [€]

$O\&M_{pipe}$  Pipelines operations and maintenance expenses [€/year]

$P$  Pressure [Pa]

$P_c$  Critical pressure [Pa]

$P_{cut-off}$  Outlet pressure of the compressor [Pa]

$P_d$  Pressure at the discharge of the compressor [Pa]

$P_{final}$  Outlet pressure of the pump [KW]

$P_{in}$  Pressure at the pipeline inlet [Pa]

$P_{initial}$  Inlet pressure of the compressor [Pa]

$P_{max}$  Maximum pressure inside the pipeline [Pa]  
 $P_{out}$  Pressure at the pipeline outlet [Pa]  
 $P_s$  Pressure at the inlet of the compressor [Pa]  
 $p_e$  Electricity cost [€/KWh]  
 $Q_m$  Average flow rate [ $kg/m^3$ ]  
 $R$  Gas constant [ $J/Kg * K$ ]  
 $Re$  Reynolds Number  
 $S$  Specific Yield Stress for the pipeline material [Pa]  
 $T_c$  Critical temperature [K]  
 $T_{in,comp}$  Temperature of  $CO_2$  at the compressor inlet [k]  
 $T_s$  Temperature at the inlet of the compressor [K]  
 $t$  Pipe wall thickness [m]  
 $V$  Volume [ $m^3$ ]  
 $V_d$  Volume at the discharge of the compressor [ $m^3$ ]  
 $V_s$  Volume at the inlet of the compressor [ $m^3$ ]  
 $v$  Average velocity inside the pipe [m/s]  
 $W$  Reversible work of compression [J]  
 $W_0$  Base scale of the compressor [KW]  
 $W_{comp}$  Total compression power [KW]  
 $W_{comp,max}$  Maximum capacity of a compressor [KW]  
 $W^{idealgas}$  Work for compressing an ideal gas [J/kg]  
 $W_{pump}$  Pumping power [KW]  
 $W_{pump,max}$  Maximum capacity of a pump unit [KW]  
 $W^{realgas}$  Work for compressing a real gas [J/kg]  
 $W_{s,i}$  Compression power at stage i [KW]  
 $y_{comp}$  Compression scaling factor  
 $y_{pump}$  Pump scaling factor

$Z$  Compressibility factor of the gas

$Z_{avg}$  Average of the compressibility factor of the gas

$Z_d$  Compressibility factor of the gas at the discharge of the compressor

$Z_i$  Compressibility factor of the gas at the inlet of the compressor

$Z_s$  Average  $CO_2$  compression power factor for each compression stage

$\gamma$  Ratio of specific heats

$\Delta P$  Pressure Drop [Pa]

$\varepsilon$  Surface roughness [m]

$\eta_{is}$  Isentropic efficiency of the compressor

$\eta_p$  Pump efficiency

$\eta_{pol}$  Polytropic efficiency

$\mu$  Dynamic viscosity of the fluid [Pa\*s]

$\mu_{mixture}$  Dynamic viscosity of the water-glycol mixture [Pa\*s]

$\rho$  Density [ $kg/m^3$ ]

$\rho_{mix}$  Density of the water-glycol mixture [ $kg/m^3$ ]

# Acronyms

ABC Ammonium Bicarbonate

AC Ammonium Carbonate

APS Announced Pledges Scenario

ASU Air Separation Unit

CAR Ceramic Auto Recovery

CCS Carbon Dioxide Capture and Storage (or Sequestration)

CCUS Carbon Dioxide Capture Usage and Storage

CO<sub>2</sub> Carbon Dioxide

EOR Enhanced Oil Recovery

EOS Equations of State

EU European Union

FEUP Faculdade de Engenharia da Universidade do Porto

GHG Greenhouse Gas

IEA International Energy Agency

IGCC Integrated Gasification Combined Cycle

IPCC Intergovernmental Panel on Climate Change

ITM Ion Transport Membrane

LCO<sub>2</sub>T Levelized Cost of Carbon Dioxide Transport

MDEA MethylDiethanolamine

MEA Monoethanolamine

NASS Non-Aqueous Solvents

O&M Operations and Maintenance

OTM Oxygen Transport Membrane

SAF Sustainable Aviation Fuels

SCPC Supercritical Pulverized Coal

STEPS Stated Policies Scenario

SwRI Southwest Research Institute

TEG triethylene Glycol

TFC Total Final Energy Consumption

# 1 Introduction

Carbon emissions, often referred to as carbon dioxide ( $\text{CO}_2$ ) emissions, stand at the forefront of global environmental concerns, exerting profound impacts on Earth's climate system and the health of ecosystems.

As the byproduct of human activities such as burning fossil fuels, deforestation, and industrial processes, carbon emissions have surged to unprecedented levels, significantly altering the planet's atmospheric composition and contributing to climate change.

Understanding the sources, impacts, and mitigation strategies surrounding carbon emissions is imperative for addressing the pressing challenge of climate change and fostering a sustainable future for generations to come. This dissertation delves into the multifaceted aspects of carbon emissions, exploring their origins, implications, and the urgent need for collective action to curb their proliferation.

It presents updated data related to global warming such as the evolution of global temperature and carbon dioxide emissions, were the emissions were separated by sector (power, industry, transport and buildings).

It was also shown the importance and necessity for carbon capture and storage (CCS) where the International Energy Agency (IEA) on its Sustainable Development Scenario (SDS) stated that the amount of carbon dioxide to be captured should evolve from the current value of 40 Megatonnes per annum to 5.6 Gigatonnes per annum until the year 2050.

After that it was done a brief comparison between the current main technologies for carbon capture.

Ending the summarized description of the main carbon capture technologies it was analysed all the aspects associated to the necessary compression and transport of  $\text{CO}_2$  from the source to the final destination.

On the  $\text{CO}_2$  transport subsection it was depicted all the characteristics associated to the four main transportation methods that are: ship, truck, rail and pipeline transport.

It was also done a general approach for performing an economical analysis on carbon dioxide transport through pipeline.

This research encompassed a study of the main aspects that affect the levelized cost of transporting  $\text{CO}_2$  (LCO<sub>2</sub>T) in pipeline such as mass flow and the pipeline length, as well as the weight that adding a booster station exerts on the global transport cost.

## 2 Literature Review

### 2.1 Climate Change

#### 2.1.1 Observed Changes and their Causes

Global warming is one of the main (if not the main) concern in our society nowadays. Human influence on the climate system is clear, and recent anthropogenic emissions of greenhouse gases are the highest in history. Recent climate changes have had widespread impacts on human and natural systems (IPCC 18).

The amount of warming caused by human activity had already risen by roughly  $1^{\circ}\text{C}$  over pre-industrial levels. In comparison to pre-industrial times (1850–1900), human activity has warmed the planet by  $0.87^{\circ}\text{C}$  ( $\pm 0.12^{\circ}\text{C}$ ) by the decade of 2006–2015. Around 2040, if the current pace of warming persists, the earth will have warmed by  $1.5^{\circ}\text{C}$  due to human activity (Figure 1) [6].

Anthropogenic greenhouse gas emissions resulted on atmospheric concentrations of carbon dioxide, methane and nitrous oxide that are unprecedented in at least the last 800,000 years (IPCC 20).

Through measurements it is clear to see that a huge part of this emissions remain "trapped" in the atmosphere (about 40 %), while the remaining share was naturally removed from the atmosphere and stored on the land (through the soil and different plants), and the ocean.

The ocean was responsible for the capture of approximately 30% of the emitted anthropogenic carbon dioxide, which resulted on ocean acidificatin as expected.

Figure 2 shows the global  $\text{CO}_2$  emissions from energy combustion and industrial processes and their annual change from 1900 to 2022. The year 2022 has set a new record in terms of emissions with an unprecedented 36.8 Gt of  $\text{CO}_2$  released [8].

Climate change is a direct consequence of this verified global warming and its effect on the different ecosystems is clear.

The alteration in precipitation and the progressive melting of the ice on different regions of the globe are all factors which affect the water resources resulting on a severe impact for terrestrial and marine species. In fact, many terrestrial, freshwater and marine species have shifted their geographic ranges, seasonal activities, migration patterns, abundances and species interactions in response to ongoing climate change (IPCC 22).

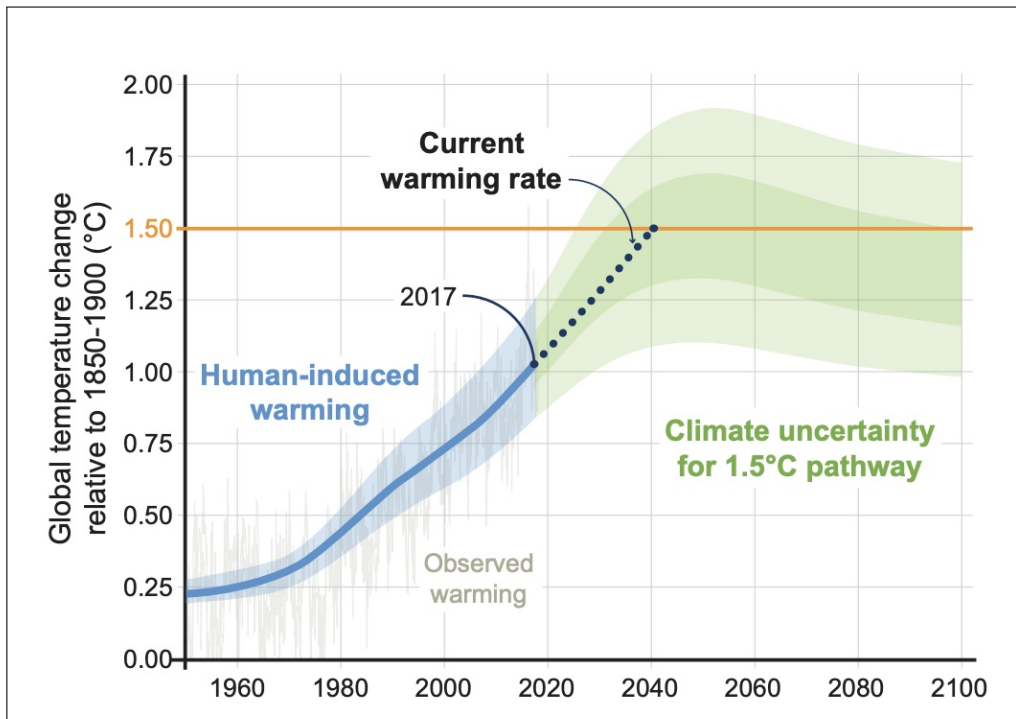


**Figure 1:** Human-induced warming reached approximately 1°C above pre-industrial levels in 2017. At the present rate, global temperatures would reach 1.5°C around 2040. Stylized 1.5°C pathway shown here involves emission reductions beginning immediately, and CO2 emissions reaching zero by 2055, [6].

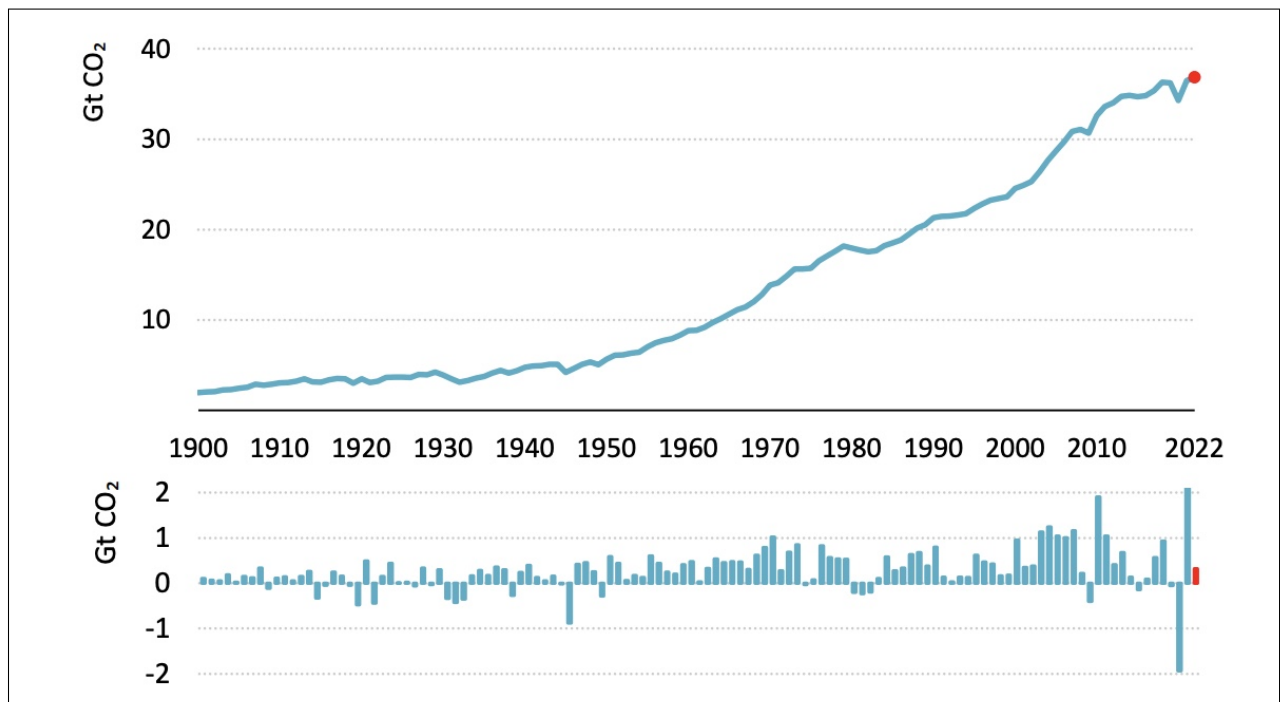


**Figure 2:** Global CO<sub>2</sub> emissions from energy combustion and industrial processes and their annual change, 1900-2022, [8].

## 2.1.2 Adaptation and Mitigation

Analysing the different paths that lead to adaptation and mitigation of all aspects associated to climate change is crucial for leading with this issue. Both scientists and engineers have come up with many different solutions however, no individual presented solution was found sufficient. Climate change specialists generally agree that solving this problem implies the simultaneous use of different technologies and solutions, with a strong presence and support from the different governments and corporations [1].

It is known that mitigation can be applied on any economic sector and its cost-effectiveness is enhanced when adopting strategies for both the reduction of energy use and greenhouse gas intensity, decarbonization of the energy supply as well as diminishing net emissions.

Sector-specific mitigation strategies are more often used to address market failures or sector-specific barriers than general economy-wide policies. They can be combined with complementing policies to form coherent packages. Administrative and political roadblocks frequently impede the adoption of economy-wide initiatives, even when they are potentially more cost-effective. The interaction of various mitigation strategies can either maximise their impact or produce no further emission reduction [1].

## 2.1.3 Total Final Energy Consumption and Emissions by Sector

According to the World Energy Outlook 2023, the current total final energy consumption (TFC) is 442 EJ, which is divided across the following end-uses: industrial (167 EJ), buildings (133 EJ), transportation (116 EJ), and other (27 EJ). This means that the transport sector which will be heavily analysed on the present dissertation accounts for nearly 26% of the TFC.

Regarding the share that each sector has on the  $CO_2$  emissions, we c

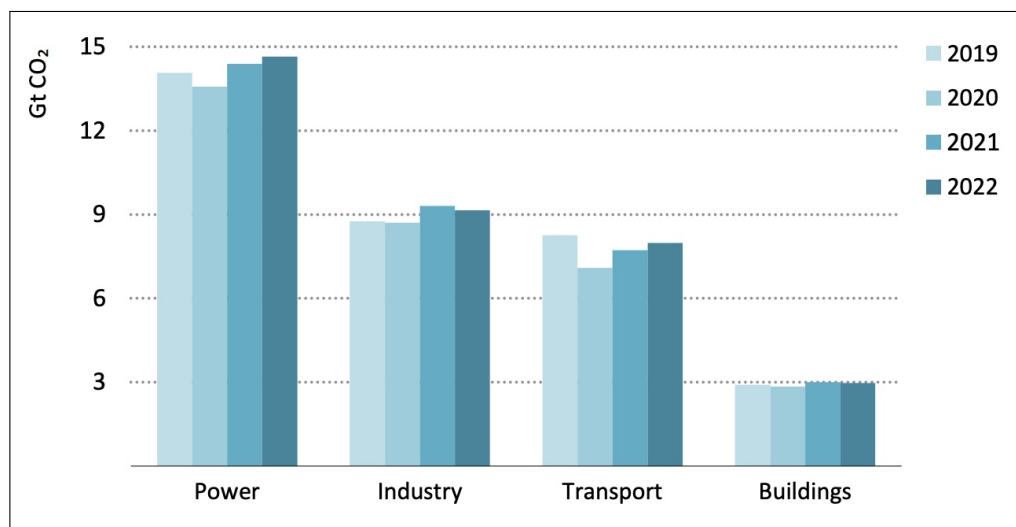


Figure 3: Global CO<sub>2</sub> emissions by sector, 2019-2022, [8].

### 2.1.4 National and EU goals for climate change mitigation

Portugal has been proactively pursuing challenging targets for reducing carbon emissions in line with larger EU aims. The Portuguese government has pledged to drastically cut greenhouse gas emissions in order to move the country towards a low-carbon, more sustainable economy. Among the main goals and projects are:

- EU ambitions: Portugal is determined to follow the EU's ambitions, which include becoming carbon neutral by 2050. This entails a significant decrease in carbon emissions in a number of economic sectors.
- Portugal has created the National Energy and Climate Plan (NECP), which lays out precise goals and plans for lowering greenhouse gas emissions, boosting the use of renewable energy sources, and improving energy efficiency. This strategy offers a road map for accomplishing the

This plan offers a road map for accomplishing the nation's climate objectives in compliance with EU laws.

**Growth of Renewable Energy:** Portugal has made large investments in the production of hydroelectric, solar, and wind energy. The nation wants to decrease its dependency on fossil fuels and the amount of carbon emissions the energy sector produces by increasing the proportion of renewable energy in its overall energy mix.

**Decarbonization of Transportation:** In an effort to lower carbon emissions from the transportation sector, Portugal is putting policies in place to support electric cars (EVs) and upgrade the infrastructure for public transit. This involves promoting sustainable mobility options, building out the infrastructure for charging EVs, and offering incentives for their purchase.

Portugal acknowledges the significance of sustainable land use and forestry management in mitigating climate change and sequestering carbon emissions. This includes rural development and forestry. Reforestation, afforestation, and sustainable land management methods are initiatives that help with carbon absorption and storage.

**International Cooperation:** Portugal is an active member of the Paris Agreement and other international climate agreements and activities aimed at mitigating climate change. The nation works with other countries to share technology, expertise, and best practices for lowering global carbon emissions.

Portugal's overall carbon emission targets are focused on moving toward a more sustainable and environmentally friendly economy while supporting international efforts to mitigate climate change. Portugal's approach to promoting innovation, investing in infrastructure for renewable energy sources, and putting effective policies into place are all crucial for achieving their ambitious goals in climate change mitigation.

## 2.2 Carbon Capture and Storage

One revolutionary tool in the fight against climate change is carbon capture and storage, or CCS. Being able to capture carbon dioxide (CO<sub>2</sub>) emissions at the source and enable substantial decreases in atmospheric CO<sub>2</sub> concentrations via removal technologies makes it an essential part of the solution.

In its Special Report on Global Warming of 1.5 degrees Celsius, the Intergovernmental Panel on Climate Change (IPCC) stressed how urgent it is to achieve net-zero emissions by mid-century in order to prevent the catastrophic effects of climate change. This requirement is reiterated in the studies performed where all possible scenarios depend on CO<sub>2</sub> removal plans in order to keep rises in global temperature to 1.5 degrees Celsius.

### 2.2.1 The need for CCS

According to the Global CCS Institute, [2], there are four main topics that justify the need for Carbon Capture and Storage which are:

- **Decarbonization in hard-to-abate industries**

Due to their heavy reliance on high-temperature heat and industrial processes, the cement, iron and steel, and chemical sectors release carbon into the atmosphere. These are among of the hardest industries to shift to low-carbon practices, thus they present serious obstacles to decarbonization efforts. Without the use of carbon capture and storage (CCS) technology, a number of reports, including those from the Energy Transition Commission and the International Energy Agency (IEA), suggest that reaching net-zero emissions in these difficult-to-abate industries may not be possible or may be significantly more expensive. Among the most tried-and-true and economical methods for reducing emissions in these industries is CCS.

- **Enabling the production of low-carbon hydrogen at scale**

In difficult industries, hydrogen is expected to be a crucial component of carbon emission reduction strategies. It has potential as a major energy source for flexible power generation and home heating. Right now, carbon capture and storage (CCS) on coal or natural gas is the most economical way to produce low-carbon hydrogen. This process is especially helpful in areas where the cost of fossil fuels is low and there is a dearth of inexpensive renewable electricity available for electrolysis-based hydrogen synthesis. By mid-century, global hydrogen production must rise significantly from 70 million tonnes per annum (Mtpa) to 425–650 Mtpa in order to decarbonize hard-to-abate industries and achieve net-zero emissions.

- **Providing low carbon dispatchable power**

Achieving net-zero emissions requires decarbonizing power generation. In addition to providing dispatchable and low-carbon electricity, power plants with carbon capture and storage (CCS) technology also perform vital grid-stabilising functions like inertia, frequency management, and voltage regulation. Wind power or solar photovoltaics (PV) are insufficient to provide these services. When combined with renewable energy sources, CCS helps build a low-carbon grid that is dependable and robust for the future.

- **Delivering negative emissions**

Compensation is necessary to address residual emissions in hard-to-abate sectors. Carbon capture and storage (CCS) is the cornerstone of technology-driven techniques for removing carbon dioxide, such as direct air capture with carbon storage (DACCS) and bioenergy with CCS (BECCS). While removing carbon dioxide is not a cure-all, the need grows more pressing every year that CO<sub>2</sub> emissions are not significantly reduced.

The International Energy Agency (IEA) created a Sustainable Development Scenario (SDS), where the amount of carbon dioxide to be captured should evolve from the current value of 40 Mt of CO<sub>2</sub> per annum to 5.6 Gigatonnes in 2050 (Figure 4). From the 5.6 Gt per annum of CO<sub>2</sub> captured, the IEA predicted a use of 369 Mtpa and a storage of 5266 Mtpa.

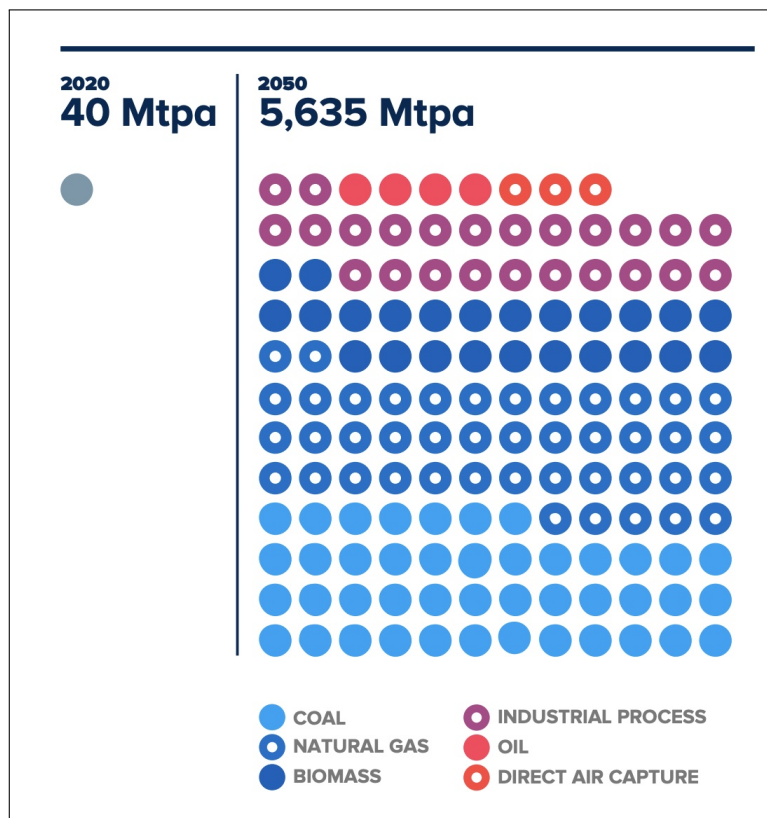


**Figure 4:** CO<sub>2</sub> CAPTURE CAPACITY IN 2020 AND 2050 BY FUEL AND SECTOR IN THE IEA SUSTAINABLE DEVELOPMENT SCENARIO, [3].

## 2.3 Technologies for Carbon capture

The development of adsorption techniques and membrane technologies in later decades has followed the early chemical and physical solvent-based approaches used in the 1930s and 1940s for carbon capture in industrial processes [10].

Carbon capture, though it originated in the natural gas industry, is becoming more and more important in reducing emissions in a variety of industries, including the power industry. However, extracting CO<sub>2</sub> from diluted gas streams has significant financial hurdles, which is why agencies such as the US Department of Energy (DOE) are launching programmes to promote cost-cutting and innovation [10].

Anticipating a 20 percent cost reduction over present solutions, second-generation technologies are expected to be used by 2025. By the 2030s, transformative technologies that aim to save thirty percent of initial implementation costs are expected to be shown. These developments have great potential to improve carbon capture's viability and scalability, which is essential for reducing global warming and promoting environmentally friendly industrial processes [10].

Technologies evolve from first observations and ideas, via bench-scale equipment and lab research, to pilot-scale and ultimately full-scale commercial service. The maturity of technologies within an increasing scale of commercial deployment is defined by a qualitative scale called the Technology Readiness Level (TRL), table 1.

**Table 1:** Simplified definitions of Technology Readiness Level (TRL) for CCS technologies, [10].

CATEGORY	TRL	DESCRIPTION
	9	Normal commercial service
Demonstration	8	Commercial demonstration, full-scale deployment in final form
	7	Sub-scale demonstration, fully functional prototype
Development	6	Fully integrated pilot tested in a relevant environment
	5	Sub-system validation in a relevant environment
	4	System validation in a laboratory environment
Research	3	Proof-of-concept tests, component level
	2	Formulation of the application
	1	Basic principles, observed, initial concept

Figures 5 and 6 represent an outlook of carbon capture technologies TRL including how they have advanced between 2014 and 2020.

TECHNOLOGY	KEY VENDORS	TRL 2014	TRL 2020	PROJECTS	
Liquid Solvent	Traditional amine solvents	Fluor, Shell, Dow, Kerr-McGee, Aker Solutions, etc	9	9	Widely used in fertilizer, soda ash, natural gas processing plants, e.g. Sleipner, Snøhvit, and used in Boundary Dam since 2014
	Physical solvent (Selexol, Rectisol)	UOP, Linde and Air Liquide	9	9	Widely used in natural gas processing, coal gasification plants, e.g. Val Verde, Shute Creek, Century Plant, Coffeyville Gasification, Great Plains Synfuels Plant, Lost Cabin Gas plant
	Benfield process and variants*	UOP	.*	9	Fertiliser plants, e.g. Enid Fertiliser
	Sterically hindered amine	MHI, Toshiba, CSIRO, etc	6-8	6-9	Demonstration to commercial plants depending on technology providers, e.g. Petra Nova carbon capture
	Chilled ammonia process*	GE	6*	6-7	Pilot tests to demonstration plant feasibility studies
	Water-Lean solvent	Ion Clean Energy, CHN Energy, RTI	4-5	4-7	Pilot test and commercial scale FEED studies: Ion Clean Energy's Gerald Gentleman station carbon capture, CHN Energy's Jinjie pilot plant
	Phase change solvents	IFPEN/Axens	4	5-6	DMX™ Demonstration
	Amino acid-based solvent*/ Precipitating solvents	Siemens, GE	4-5	4-5	Lab test to conceptual studies
	Encapsulated solvents	R&D only	1	2-3	Lab tests
	Ionic liquids	R&D only	1	2-3	Lab tests
Solid adsorbent	Pressure Swing Adsorption/Vacuum Swing Adsorption	Air Liquide, Air Products, UOP	3	9	Air Products Port Arthur SMR CCS
	Temperature Swing Adsorption (TSA)	Svante	1	5-7	Large pilot tests to FEED studies for commercial plants
	Enzyme Catalysed Adsorption	CO <sub>2</sub> solutions	1	6	Pilot demonstrations
	Sorbent-Enhanced Water Gas Shift (SEWGS)	ECN	5	5	Pilot tests, e.g. STEPWISE
	Electrochemically Mediated Adsorption	R&D only	1	1	Lab test

Figure 5: TRL assessment and key technology vendors of the CO2 capture technologies, [10].

TECHNOLOGY		KEY VENDORS	TRL 2014	TRL 2020	PROJECTS
Membrane	Gas separation membranes for natural gas processing	UOP, Air Liquide	-*	9	Petrobras Santos Basin Pre-Salt Oil Field CCS
	Polymeric Membranes	MTR	6	7	FEED studies for large pilots
	Electrochemical membrane integrated with MCFCs	FuelCell Energy	-*	7	Large pilots at Plant Barry
	Polymeric Membranes / Cryogenic Separation Hybrid	Air Liquide, Linde Engineering, MTR	6	6	Pilot studies
	Polymeric Membranes/ Solvent Hybrid	MTR/ University of Texas	-*	4	Conceptual studies
	Room Temperature Ionic Liquid (RTIL) Membranes	R&D only	2	2	Lab tests
Solid-looping	Calcium Looping (CaL)	Carbon Engineering	6	6-7	Feasibility/cost studies for commercial scale
	Chemical Looping Combustion	Alstom	2	5-6	Pilot tests
Inherent CO <sub>2</sub> capture	Allam-Fetvedt Cycle	8 Rivers Capital	2	6-7	50 MW Demonstration Plant in La Porte
	Calix Advanced Calciner*	Calix	-	5-6	Large pilot LEILAC

Figure 6: TRL assessment and key technology vendors of the CO2 capture technologies, [10].

### 2.3.1 Pre-combustion Capture

For many years, the chemical, oil, and gas sectors have been extracting CO<sub>2</sub> from gas streams. Most of the time, the removal of CO<sub>2</sub> is necessary to meet the specifications for the downstream products—whether they be chemicals, hydrogen, or natural gas.

Pre-combustion capture is a term that has gained a lot of traction in the context of gasification-based power plants, especially IGCCs. These plants are designed to convert gas produced through gasification (henceforth referred to as "syngas") into hydrogen and CO<sub>2</sub>, and to remove CO<sub>2</sub> from the syngas stream before the hydrogen-rich gas in the gas turbine is burned. This is done in anticipation of regulations aimed at limiting CO<sub>2</sub> emissions [4].

#### Pre-Combustion Capture Technology

Currently, the final CO<sub>2</sub> capture in natural gas processing, natural gas reforming, gasification, and IGCC is achieved under pressure using an acid gas removal (AGR) process that involves solvent

absorption followed by regenerative stripping of the rich solvent to release the  $\text{CO}_2$ . The  $\text{CO}_2$  can then be compressed and sent to sequestration or supplied for EOR. Chemical and physical solvents are the two main categories of "acid gas" ( $\text{CO}_2$ ,  $\text{H}_2\text{S}$ , and  $\text{COS}$ ) removal (AGR) solvents [4].

- Chemical Absorbents

This type of absorbents react with the acid gases separating them through the reverse of their reactions. This reverse process is achieved by using big quantities of heat. Compared to physical solvents, these procedures often require less capital for AGR, but they also require more steam heat to regenerate the solvent [4].

Some examples of Chemical Absorbents are specific types of amines such as MDEA.

- Physical Absorbents

The process of AGR through physical absorbents starts by dissolving the acid gas at high levels of pressure. After which it is eliminated from the solvent from a decrease in pressure and consequent increase in temperature. These type of absorbents require less steam-heat for solvent regeneration when comparing with chemical solvents. The process which uses Rectisol has a higher cost but leads to the best removal of the acid gas [4].

The acid gas removal process of an IGCC plant consists of two different absorber/stripper pairs. One is responsible for removing the  $\text{H}_2\text{S}$  rich stream and the other removes  $\text{CO}_2$  from the sulphur free gas stream. The  $\text{H}_2$  rich syngas is then delivered to the gas turbine power block. The solvent rich in  $\text{CO}_2$  is sent to a stripper for solvent regeneration being the remaining stripped  $\text{CO}_2$  dried and compressed in order to achieve appropriate transportation and storage conditions [4] (Figure 5).

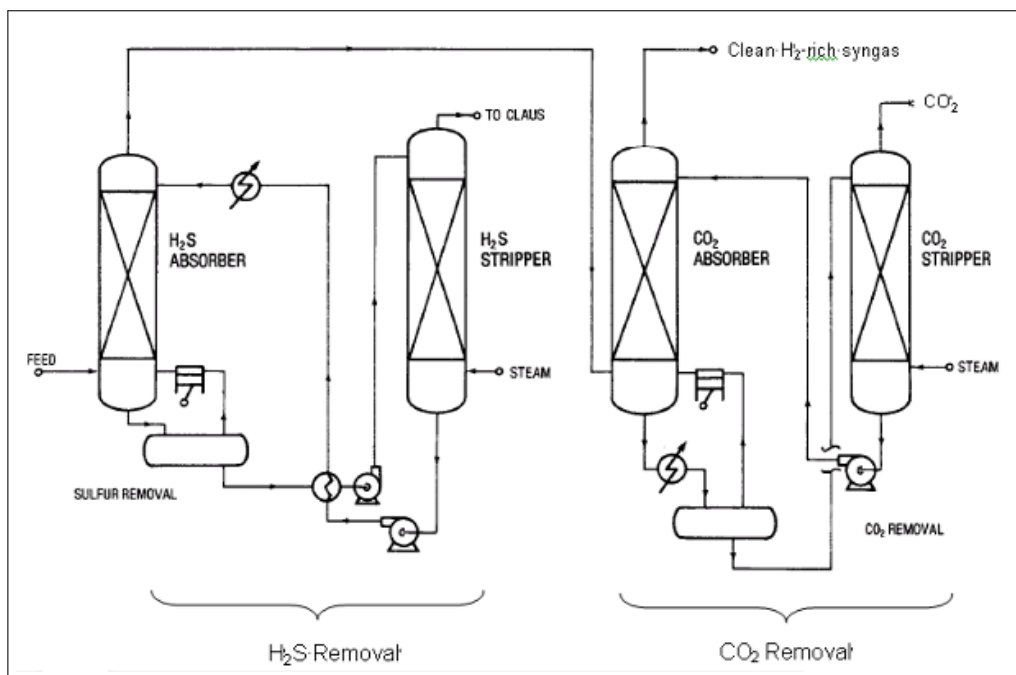


Figure 7: Typical IGCC AGR Process Arrangement for  $\text{CO}_2$  Capture , [4].

### 2.3.2 Post-Combustion Capture

There are several ways to do post-combustion capture (PCC) of CO<sub>2</sub> from flue gases, including membranes, adsorption, physical and chemical absorption.

#### SOLVENT-BASED CO<sub>2</sub> CAPTURE

It is not a novel procedure to extract CO<sub>2</sub> from industrial gas streams. The natural gas industry has been employing chemical solvents-based gas absorption techniques to extract CO<sub>2</sub> from other gases since the 1930s. Separation is made easier by the fact that natural gas usually has substantially higher CO<sub>2</sub> concentrations than gases produced during combustion [9].

The main technologies available for solvent-based CO<sub>2</sub> capture are: amines, non-aqueous solvents (NASS), carbonate-based solvents, phase change solvents and catalyzed processes. The applicability of each technology is mainly dependant on the partial pressure of acid gas in both the feed and the resulting product i.e, the treated flue gas (Figure 6).

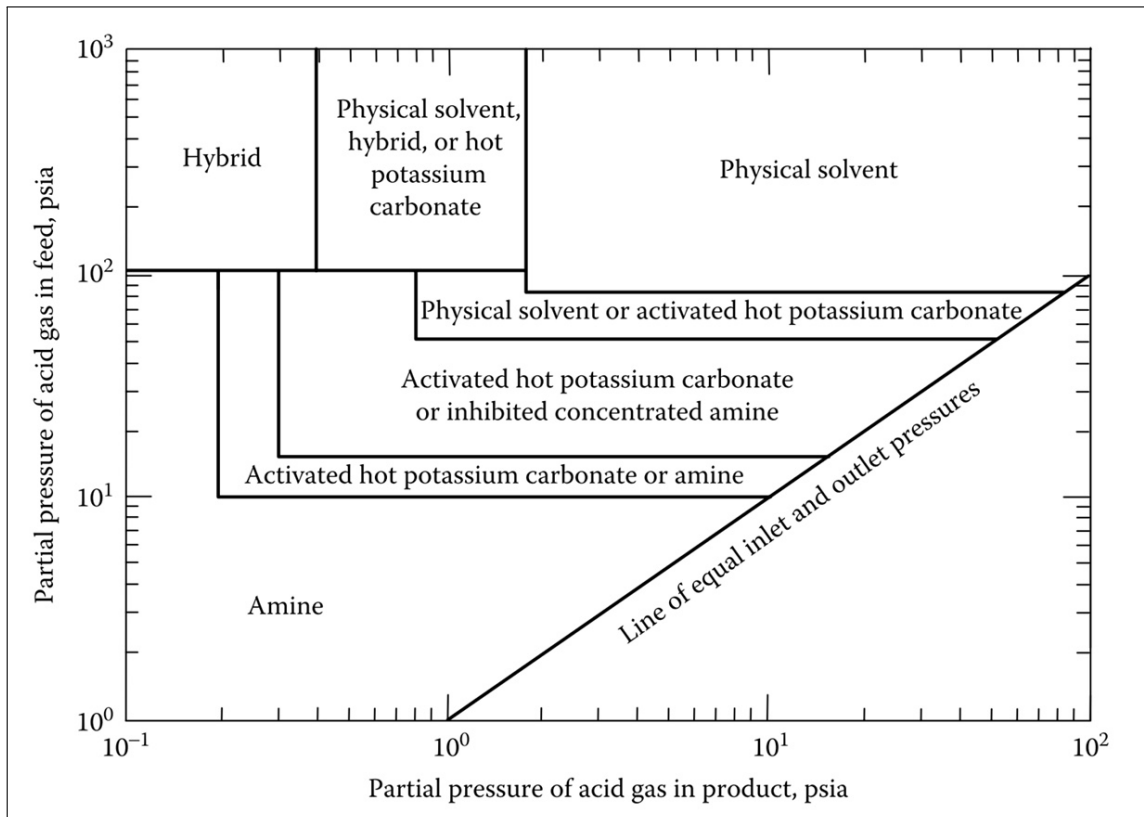


Figure 8: Chart for Selecting CO<sub>2</sub> Removal Technologies Available Commercially , [9].

Chemical solvent absorption, such that found in amine types, is a tried-and-true technology that regularly and dependably performs in numerous applications. It is used to produce hydrogen and sweeten natural gas. Currently, the most economical way to directly obtain high purity CO<sub>2</sub> is through the reaction of CO<sub>2</sub> with amines.

The power plant's flue gases are cooled and treated to remove particles, SO<sub>x</sub>, and NO<sub>x</sub>. Subsequently, the exhaust gases travel via an absorber after being given an extra boost by a fan to

counteract system pressure dips. In order to absorb the CO<sub>2</sub>, a lean amine solution interacts with the exhaust gases countercurrently [5].

The stack is where the clean flue gases go next. To separate the amine from the CO<sub>2</sub>, the CO<sub>2</sub> rich amine solution is fed into a stripper, also known as a regenerator. Steam provides the energy needed to adsorb the CO<sub>2</sub> from the solution. After condensing the CO<sub>2</sub>-rich solution at the top of the stripper to remove water, the gaseous CO<sub>2</sub> is transported for additional drying and compression [5].

The main characteristics of amines that make them suitable candidates for post-combustion flue gas CO<sub>2</sub> capture are:

- **Quick reaction with CO<sub>2</sub>:** The size of the absorber required to extract a specific amount of CO<sub>2</sub> from the entering flue gas largely determines the cost of CO<sub>2</sub> capture. If the solvent can absorb CO<sub>2</sub> more quickly, it can be separated from the flue gas with a smaller absorber volume, which reduces the cost of capture. Faster solvent kinetics lead to greater mass-transfer performance as long as other factors are not impeding CO<sub>2</sub> transfer across the gas-liquid interface [9].
- **Large net-CO<sub>2</sub> carrying capacity:** The regeneration load, auxiliary unit costs, and energy requirements are all determined by the amount of solvent required to extract CO<sub>2</sub> from the flue gas. Solvents must be able to carry large amounts of CO<sub>2</sub> [9].
- **Low-enthalpy of reaction with CO<sub>2</sub>:** Energy is needed to break the amine-CO<sub>2</sub> bond in order to desorb CO<sub>2</sub>, as amines and CO<sub>2</sub> react chemically. Compared to tertiary amines, which generate carbonates, primary and secondary amines that form carbamates have a higher enthalpy of reaction with CO<sub>2</sub> [9].
- **Minimal energy loss when heating and vaporising water:** In aqueous solutions, amines are often utilised in concentrations ranging from 30 to 50 weight percent. Water evaporation raises the energy penalty, the useless load, and the steam requirements due to its high latent heat of vaporisation.

Reducing the water content in solution increases the CO<sub>2</sub> carrying capacity as well as the energy lost to evaporate the water; however, this also raises the viscosity of the solution and may accelerate corrosion. The maximum amine concentration that is practical for solvent processes is usually used when viscosity, corrosion, carbamate precipitation, and column temperature bulge problems are either negligible or well under control [9].

Generally speaking, tertiary amines react with CO<sub>2</sub> at a slower pace than primary and secondary amines. Since MEA has the highest reaction rate of any primary amine, it is commonly employed in blends with other tertiary or hindered amines to take advantage of this property while keeping reboiler loads relatively low. MEA is extremely biodegradable and has no direct negative effects on the health of people, animals, or vegetation from the standpoint of environmental and health safety [9].

Figure 7 represents a schematic of the amine-based CO<sub>2</sub> capture technology with MEA.

Following the removal of traditional air pollutants (SO<sub>x</sub>, NO<sub>x</sub>, and PM), the combustion flue gas travels countercurrently to a CO<sub>2</sub>-lean solvent where CO<sub>2</sub> is absorbed and interacts with the MEA to generate chemicals that are soluble in water [9].

When the CO<sub>2</sub>-rich solution is fed to a stripper reactor for regeneration, the treated flue gas—which is primarily N<sub>2</sub>—is released into the environment. The CO<sub>2</sub>-rich solution in the stripper is heated to dissolve the salt and replenish the MEA solvent. The heat required for the regeneration of the MEA solvent in the stripper is supplied by a reboiler using steam that is taken from the turbine cycle [9].

As a result, the stripper releases CO<sub>2</sub>, creating a concentrated stream that emerges and is then cooled and dehumidified in order to be ready for compression, transportation, and storage. The CO<sub>2</sub>-lean solution is removed from the stripper, cooled, and then put back into the absorber for further usage [9].

Carbon-capture technologies that use MEA nowadays are based on solvent concentrations of 20% and 30% diluted on water. Being the absorption stage of the process exothermic, the large share of water present on the solution helps in controlling the solvent temperature during this stage [9].

However, this type of solvent concentrations have an important disadvantage which relates to the water high values of sensible heating and stripping energy when regenerating the CO<sub>2</sub>. Typical MEA systems have an energy consumption that can go anywhere from 3.6 to 7 GJ/T CO<sub>2</sub> in the form of low-pressure steam which is necessary for the regeneration of the solvent in order to generate a concentrated CO<sub>2</sub> stream at approximately 1.7 bar [9].

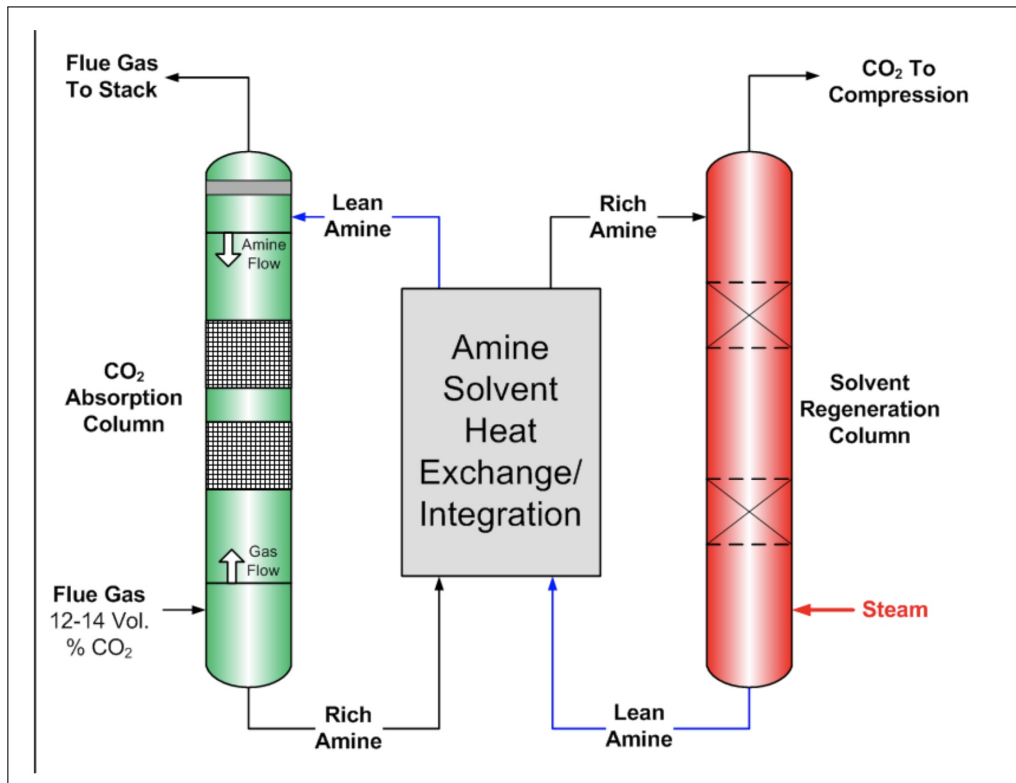


Figure 9: Schematic of Amine-Based Post-Combustion CO<sub>2</sub> Capture Process, [9].

## SORBENT-BASED CO<sub>2</sub> CAPTURE

There are two main ways of applying the adsorption mechanism: either by physical adsorption (physisorption) or by chemical adsorption (chemisorption).

Despite the existence of many well-established uses of sorbents for CO<sub>2</sub> capture, sorbent-based CO<sub>2</sub> capture is typically not preferred over solvent and membrane-based technology for industrial-scale carbon capture applications. This suggests that, in many or most cases, sorbent-based technology is simply not as cost-effective as solvent or membrane-based separation alternatives [9].

The main challenges associated with sorbent-based CO<sub>2</sub> capture are the following, [9]:

- High cost of many sorbents is high (i.e., particularly zeolites)
- CO<sub>2</sub> adsorption capacity limitations
- Operation at higher flue gas/exhaust gas temperatures
- Sorbent attrition
- Sorbent regeneration (energy demands)

Potential benefits of a solid sorbent post-combustion CO<sub>2</sub> capture technology over a traditional aqueous solvent-based method like monoethanolamine (MEA) include the following:

- Energy penalty: Compared to solvents, solid sorbents have the ability to greatly lower the regeneration energy penalty. This reduction in the energy penalty can be attributed to two factors: (1) solids have a significantly lower heat capacity than water (by about a factor of four), which drastically lowers the sensible heat input needed to accomplish the temperature swing; and (2) solids will have a significantly lower moisture content during regeneration than solvents, meaning less evaporation will occur [9].
- Range of operating temperature: The temperature range in which aqueous solvent-based processes can operate is constrained. On the other hand, a variety of solid sorbent kinds are available that enable use at temperatures as high as 700 °C [9].
- Miscellaneous benefits: During cycling, solid sorbents produce less waste, and their disposal is made easier by the fact that used solid sorbents have a smaller environmental impact than solvents [9].

In regards to sorbent classification, they can be divided in 3 categories, [9]:

- Low temperature (<200°C), e.g. Solid amine-based adsorbents and Carbon-based adsorbents;
- Intermediate temperature (200–400 °C), e.g. Layered double hydroxide (LDH)-based sorbents;
- High temperature (>400 °C), e.g. CaO-based sorbents.

The power plant efficiency and energy penalty associated to sorbent-based CO<sub>2</sub> capture have been considerably improved but there is still the need for a cut on both capital costs and operating costs.

In fact, there is a need for improvement regarding the following aspects:

- Sorbent performance under realistic conditions: The issues of sorbent stability in humid flue gas streams with low CO<sub>2</sub> partial pressure have already been partially addressed in the past, but more work is needed to ensure practical operation in real-world settings. Lower capacities and reaction kinetics in CO<sub>2</sub> uptake and regeneration may be exhibited by more stable sorbents, resulting in increased capital expenditures for process equipment [9].
- Costs of advanced sorbents: Because they are unique technologies, advanced sorbents are unique and their materials costs are typically much higher than those of standard CO<sub>2</sub> capture technologies (amine solvent-based). Improvements in feedstock cost reduction are required, as well as lower manufacturing process costs achieved through enhanced synthesis, economies of scale, etc [9].
- Operability concerns: These comprise understanding and controlling emissions related to new sorbent-based processes, sorbent degradation, and solids handling challenges unique to sorbent-based processes that are not encountered in traditional solvent-based technologies [9].

## MEMBRANE-BASED CO<sub>2</sub> CAPTURE

Gases like CO<sub>2</sub> can be separated by membrane using variations in the relative transfer rates or permeation of different gases through a barrier. The degree of gas separation can be adjusted depending on the relative diffusivity and surface adsorption of the different gases present. For various membrane materials, including polymers, metals, and ceramics, there are differences in the precise mechanisms for adsorption and transport. Figure 10 displays the relative permeabilities of different gas species in the polymer polydimethylsiloxane to provide an example [9].

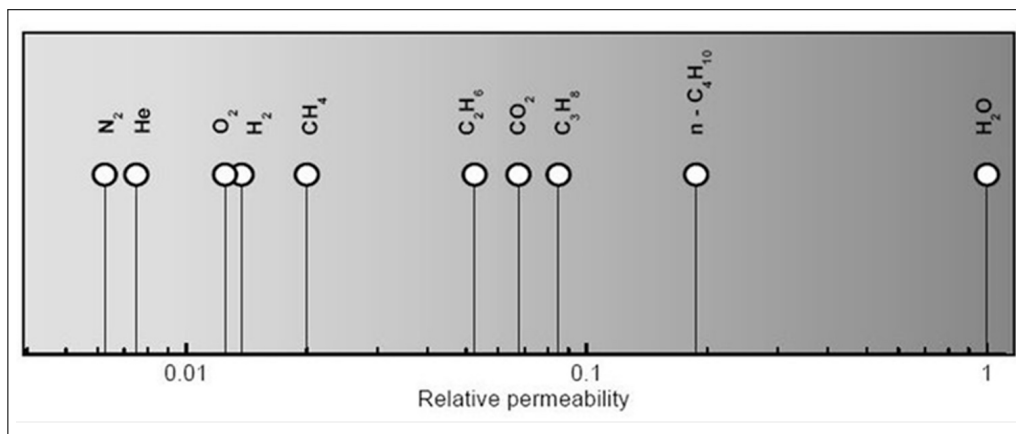


**Figure 10:** Relative Permeabilities of Gases in Polydimethylsiloxane, [9].

The feed gas is injected into a membrane unit or module and comes into contact with the membrane surface in membrane-based gas separations. The molecular species that penetrates through the membrane and comes into touch with its surface is known as the penetrant or permeant. The

stream that exits the membrane module and contains penetrants is known as the permeate. The stream that exits the membrane module without going through the membrane when it has run out of one or more penetrants is known as the non-permeate or retentate [9].

For better understanding the membrane-based CO<sub>2</sub> capture process, it is crucial having a clear notion of the following concepts, [9]:

- Permeability: Transport flux per unit trans-membrane driving force per unit membrane thickness. SI units: [kmolm/m<sup>2</sup>-s-kPa];
- Permeance: Transport flux per unit trans-membrane driving force; permeance equals permeability divided by membrane thickness. SI units: [kmol/m<sup>2</sup>-s-kPa];
- Selectivity: Ratio of the permeability or permeance of one component to another for a given membrane material at stated conditions.

Greater purity of the CO<sub>2</sub> that is caught and high membrane permeability reduce the needed membrane area, which makes higher selectivity values desirable. This is a serious problem because permeance and selectivity typically have an inverse relationship; that is, the more selective a membrane is for any given pair of gases, the lower its permeance [9].

The desired gas in the permeate is diluted for high permeance membranes, but significantly more membrane area is required for high selectivity membranes, where the desired gas is relatively concentrated. Even yet, the cost of manufacturing a membrane with high permeance and great selectivity might be unrealistic [9].

While membrane-based CO<sub>2</sub> capture technology is still relatively new in the commercial industry, it has the potential to provide a number of benefits over traditional aqueous solvent-based processes, including monoethanolamine (MEA) in post-combustion CO<sub>2</sub> capture, such as [9]:

- Simple operation; no chemical reactions, no moving parts, no heating/temperature swing required to recover CO<sub>2</sub>, no use of hazardous chemicals;
- Tolerance to high levels of wet acid gases (for certain membrane types), i.e. inert to oxygen;
- Compact and modular with a small footprint (at least at lower capacities) and easily scalable;
- Potential for inherent energy efficiency (aprox.20% plant energy at 90% capture);
- No additional water used (and in most configurations recovers water from flue gas).

Besides these clear benefits, most membrane-based CO<sub>2</sub> capture technologies also have the advantage of not requiring steam, which is the case for the regeneration stage necessary on both solvent and sorbent based technologies. Which means that there is no need for modifying existing boilers and steam turbines, [9].

The current capability of membranes for commercial large-scale CO<sub>2</sub> capture is limited, indicating that competing methods are typically more cost-effective. This is the result of some challenges faced by this type of technology such as:

- The current membranes' permeability and permeability are not as good as they could be (see the following section for further details). huge membrane areas emerge from this, necessitating huge, awkward membrane module footprints and significant capital expenditures (for the membrane and module housings). Reduced membrane area is dependent on high CO<sub>2</sub> permeance, or H<sub>2</sub> permeance in some pre-combustion capture systems, [9];
- Utility steam is typically not required for membrane separations, but it is frequently required to create the driving force for separation with a significant compression or vacuum capacity. Compressors and vacuum pumps require costly auxiliary electricity to operate, which lowers the power plant's net electrical generation. It is crucial to cut costs by using more effective process configurations and methodologies, [9];
- In post-combustion and pre-combustion membrane-based capture setups, respectively, potential hazardous pollutants (fly ash, SO<sub>2</sub>, NO<sub>x</sub>, water, and trace metals in flue gases; H<sub>2</sub>S, ammonia, fly ash, and trace metals in syngas) may shorten the lifetime and effectiveness of membranes/modules, [9];
- The implementation of membrane-based CO<sub>2</sub> collection systems is hindered by technological and financial risk, which is exacerbated by the lack of experience operating these systems, especially at the scales associated with large coal-fueled facilities, [9].

In regards to the membrane module design, figure 11 shows a schematic representation of the four most used membrane designs. Tubular and plate-and-frame designs are common in filtration and water treatment applications. Multiple tubes are often packed into a single cylindrical vessel. This is referred to as a shell-and-tube design. Currently, all industrial, gas separation membrane applications employ polymer membrane technology based on hollow fibers or flat sheets, [9].

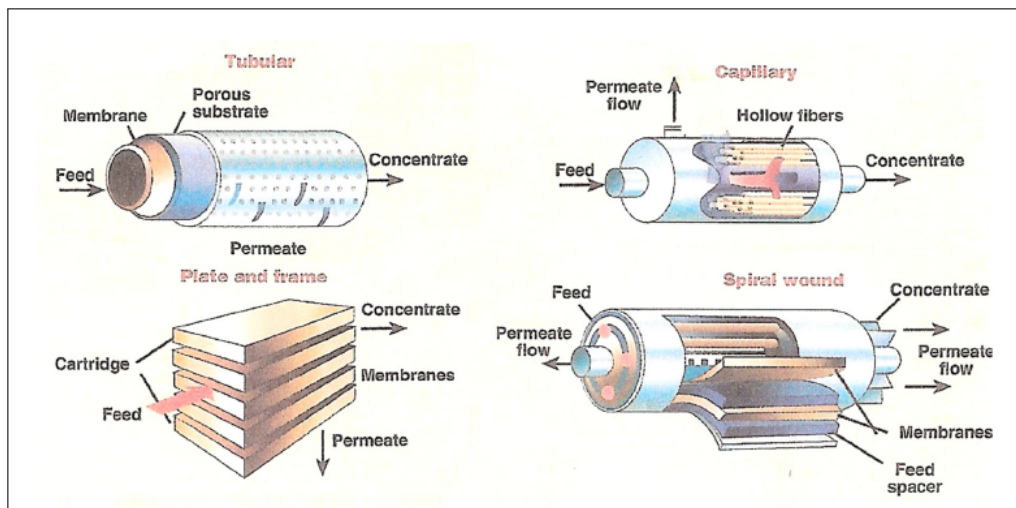


Figure 11: Common Membrane Module Designs, [9].

Finally, classifying the membranes suitable for CO<sub>2</sub> separation by type, we can highlight the following, [9]:

- Polymeric membranes (e.g., polyethyleneoxide, polydimethylsiloxane, sulphonated polyimides)

- Ceramics (aminosilicate structures)
- Supported liquid membranes (facilitated transport)
- Metallic membranes (e.g., palladium, palladium alloys for hydrogen separation)
- Other (zeolites, etc.)

### 2.3.3 Oxy-Combustion Capture

An oxygen-combustion power plant produces extremely pure carbon dioxide (CO<sub>2</sub>) exhaust that can be inexpensively and permanently stored since oxygen, not air, is used to burn fuel.

In order to control burning and raise the flue gas's carbon dioxide content, oxygen is frequently combined with the gas. Because nitrogen in the air is not included in the flue gas and because there is about 75% less flue gas produced during combustion of oxygen than during air in the Rankine Steam Cycle, the volume of flue gas exiting the boiler is significantly smaller than that of conventional airfired combustion. The flue gas is mostly composed of carbon dioxide [5].

The procedure makes use of an air separation unit (ASU), a device with a significant electrical consumption need.

New and less energy-intensive oxygen separation technologies, such as ion transport membranes (ITM), oxygen transport membranes (OTM), and BOC's ceramic auto thermal recovery (CAR) oxygen generation method, are being developed to lessen the auxiliary load. Other promising coupled cycles utilising gas and steam turbines are also linked to oxy-combustion [5].

Two such cycles that are now being studied theoretically are the semi-closed oxy-combustion mixed cycle and the Grab cycle. This idea of oxy-combustion can be used with methane, syngas, or biomass gasification, among other fuels [5].

## 2.4 The Transport Sector

According to the Stated Policies Scenario (STEPS) that has a point of view resulting from the latest policy settings, including energy, climate and related industrial policies, the global car fleet is expected to increase by over 15% until the year 2030. Considering the same time line, the activity related to aviation is expected to double, the rail passenger-kilometres will increase by 36% and the shipping tonne-kilometres will have an increase of 20% [7].

The Announced Pledges Scenario (APS) assumes all national energy and climate targets made by governments are met in full and on time. This implies making a reduction on private transportation leading to rail passenger-kilometres being over 5% higher in 2030 than in the STEPS scenario [7].

Finally, the Net Zero Emissions by 2050 (NZE) Scenario which limits global warming to 1.5°C considers stronger measures to cut emissions reducing the activity in aviation by 20% and the car stock by 15% in comparison to the STEPS scenario in 2050 [7].

Aviation accounts for over 2% of energy-related emissions and up until 2050, it is anticipated that rising aviation demand would result in an annual rise in flight activity of about 4%. This indicates that the creation and use of lower carbon fuels is urgently needed [7].

Sustainable Aviation Fuels (SAF) have the potential to replace oil and cut emissions however, their current cost makes them responsible for less than 0.01% of the energy used in flight. They are drop-in fuels that can be blended with traditional oil products at rates of up to 50%, whether they come in the form of synthetic or biojet kerosene. Bio-kerosene production currently costs twice as much as conventional kerosene, and synthetic kerosene four-times more [7].

According to the STEPS, biojet kerosene will account for 2% of aviation’s total energy requirement in 2030 and 6% in 2050, as opposed to over 5% and 37% in the APS and 11% and 70% in the NZE Scenario (Figure 12) [7].

The NZE Scenario’s need for synthetic kerosene in 2050 is almost twice as high as the APS’s. The greater levels of demand in the APS and the NZE Scenario are predicated on larger industry investments and government support for SAF within the framework of more comprehensive policy frameworks that prioritise emission reduction [7].

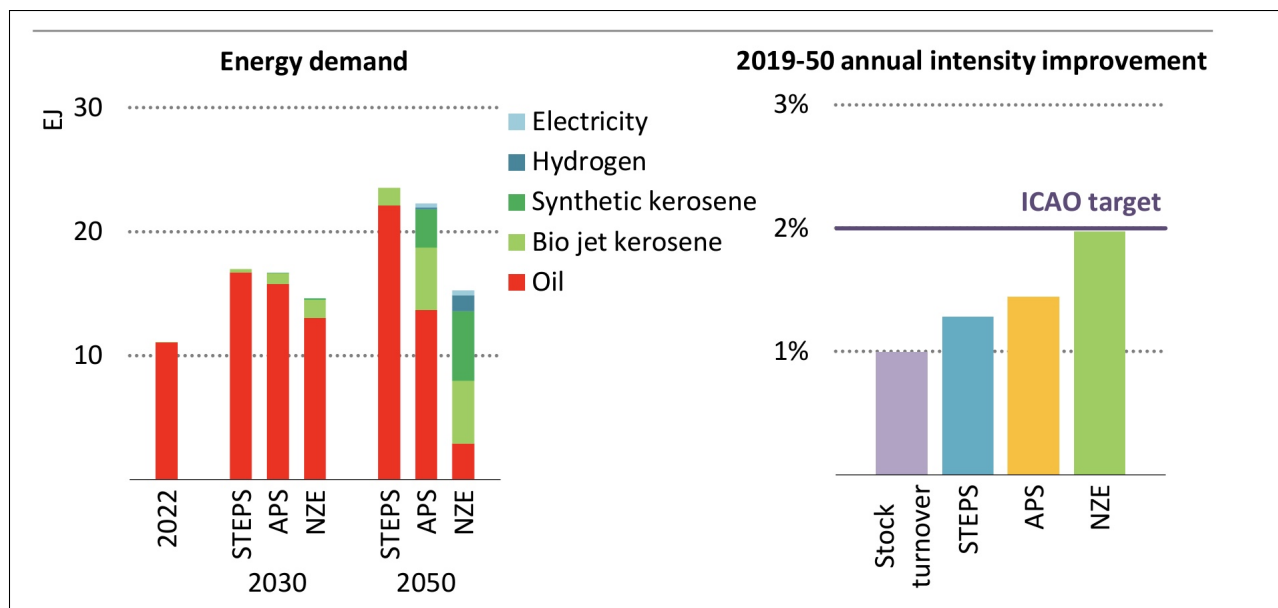


**Figure 12:** Energy demand in aviation by fuel and scenario, 2022-2050, and annual fuel intensity improvement rate, 2019-2050, [7].

Alternative production paths utilising resources including municipal solid waste and agricultural and forestry residues must be commercialised in order to meet future increases in demand for biofuels [7].

For the development and commercialization of SAF technologies, such as synthetic kerosene, which now have high prices and little technological readiness, both public and private funding are required [7].

### 2.4.1 National and EU goals for the implementation of synthetic fuels on the transport sector

Portugal has not made public any clear plans for implementing synthetic fuels, sometimes referred to as e-fuels or synthetic fuels, in the country's transportation sector. But it's crucial to remember that synthetic fuels offer an important route to cut carbon emissions in the transportation sector, especially in industries like aviation, heavy-duty transportation, and maritime shipping where electrification may be difficult.

EU however has set high standards for the use of synthetic fuels, sometimes referred to as e-fuels or synthetic fuels, in the transportation sector. The objectives and programs of the EU concerning synthetic fuels are as follows:

- **EU's Renewable Energy Directive (RED II):** Sets targets for the percentage of renewable energy in the transportation sector, including the use of renewable fuels like synthetic fuels. By 2030, member states must raise the proportion of renewable energy in transportation to at least 14%, with separate goals for advanced biofuels and renewable fuels originating from non-biological sources, such as synthetic fuels.
- **European Green Deal:** The EU's comprehensive plan for attaining carbon neutrality by 2050 is outlined in the 2019 announcement of the European Green Deal. One promising technique for cutting carbon emissions in hard-to-abate industries like shipping and aviation is synthetic fuels. In its pursuit of a climate-neutral economy, the EU intends to promote synthetic fuels research, development, and use.
- **European Clean Hydrogen Alliance:** The European Union established the European Clean Hydrogen Alliance with the aim of expediting the advancement and implementation of clean hydrogen technologies, encompassing the manufacturing of synthetic fuels derived from hydrogen. Synthetic fuels derived from hydrogen that are made from low-carbon hydrogen or renewable energy sources are considered to be essential to the EU's decarbonization of industry and transportation.
- **Research, Innovation, and Investment:** Through initiatives like Horizon Europe and the Innovation Fund, the European Union (EU) finances and supports research, innovation, and investment in synthetic fuel technology. These programs seek to increase efficiency, create more affordable production methods, and expand the use of synthetic fuels in the transportation industry.
- **Regulatory Framework:** To make it easier to produce, certify, and utilize synthetic fuels in the transportation industry, the EU is creating a regulatory framework. To make sure that synthetic fuels support general decarbonization efforts and do not worsen environmental effects, this includes sustainability, carbon intensity, and lifecycle emissions criteria.

In general, the European Union acknowledges that synthetic fuels have the potential to significantly contribute to the decarbonization of the transportation sector and the accomplishment of its climate goals. As part of a larger shift to a sustainable, low-carbon economy, the EU seeks to assist the research and deployment of synthetic fuels through legislative measures, financing programs, and strategic initiatives.

### 3 $CO_2$ Compression and Transport

Compressed  $CO_2$  must be transported via pipeline for geologic storage, increased oil recovery, or  $CO_2$  usage once it has been extracted from coal flue gas or synthesis gas. In addition to the energy needed to separate  $CO_2$  from flue gas, compression constitutes a considerable parasitic burden [9].

The compression of  $CO_2$  is difficult due to its high gas volumetric flow rate, high pressure ratio (about 100:1), and significant fluctuations in its physical characteristics within its critical temperature and pressure range [9].

In this case, developing cutting-edge compression technologies that can drastically reduce the capital and operating costs is necessary to reduce the cost of capture (as well as the cost of power) [9].

#### 3.1 $CO_2$ Compression

Equation 3.1.1 that follows gives the reversible work necessary for compressing a fluid in a closed system without flow.

$$W = \int_{V_s}^{V_d} P dV \quad (3.1.1)$$

The variable  $P$  represents the pressure, and  $V$  the volume. The reversible work for compression in open systems, where fluid enters and exits a control volume, must also take the flow work into consideration. It is written as:

$$W_{reversible} = \int_{P_s}^{P_d} V dP \quad (3.1.2)$$

The volume of a compressible fluid changes dramatically as pressure increases. Two extremes of the gas compression spectrum are represented by adiabatic compression, in which the fluid does not lose heat to its surroundings, and isothermal compression, in which the fluid is in thermal equilibrium with its surroundings [9].

Because the gas temperature does not change between the compressor's inlet and output, isothermal compression requires less work because the system's work, that is the change in enthalpy, is not wasted when the gas's sensible heat increases [9].

The fluid's entropy remains constant from the input to the output of a reversible adiabatic (isentropic) compression operation.  $PV^\gamma = \text{constant}$ , where  $\gamma = C_p/C_v$  is the ratio of specific heats at constant pressure and constant volume, respectively, for an ideal gas undergoing adiabatic compression [9].

More often than not, multi-stage centrifugal compressors use polytropic processes, which are

characterised by the following relation:  $PV_{pol}^n$  is equal to constant, where the polytropic exponent is denoted by  $n_{pol}$ . The polytropic efficiency ( $\eta_{pol}$ ) and gas characteristics determine the polytropic exponent ( $n_{pol}$ ) [9].

A path that exhibits a constant ratio of reversible work input to enthalpy rise is known as a polytropic process. An infinite series of isentropic (constant entropy) compression steps, each followed by an isobaric (constant pressure) heat addition, is what is known as a polytropic process. Because of the nature of this reversible heat addition, the temperature increase it produces is equal to that caused by the irreversible losses in the actual process [9].

The compressor's inlet capacity determines the polytropic efficiency, which is set by the manufacturer. The relationship between  $\eta_p$  and the ratio of specific heats ( $\gamma$ ) for an ideal gas is as follows:

$$\eta_{pol} * \frac{(n - 1)}{n_{pol}} = \frac{\gamma - 1}{\gamma} \quad (3.1.3)$$

If  $n$  is known, the work for compressing an ideal gas in a polytropic process can be estimated by integrating VdP from  $P_s$  to  $P_d$  and is represented as [9]:

$$W^{idealgas} = H_R^{idealgas} = \frac{H_p^{idealgas}}{\eta_{pol}} = \left[ \frac{8.314}{MolWt} \right] \left[ \frac{n_{pol}}{n_{pol} - 1} \right] \frac{T_s}{\eta_{pol}} \left[ \left( \frac{P_d}{P_s} \right)^{\frac{n_{pol}-1}{n_{pol}}} - 1 \right] \left[ = \right] \frac{KJ}{Kg} \quad (3.1.4)$$

In this equation,  $H_p^{idealgas}$  represents the polytropic head for compressing the ideal gas,  $H_R^{idealgas}$  is the actual (effective) head to compress the ideal gas, MolWt is the molecular weight and  $T_s$  is the temperature of the gas at the inlet of the compressor [9].

The ideal gas law,  $PV = RT$  (for one mol of gas), is no longer applicable at high pressures due to the intense interactions between molecules. The compressibility factor can be used to modify the ideal gas polytropic work in order to account for this departure from ideal gas behaviour [9].

$$W^{realgas} = H_R^{realgas} = \frac{H_p^{realgas}}{\eta_{pol}} \approx \left[ \frac{8.314}{MolWt} \right] \left[ \frac{n_{pol}}{n_{pol} - 1} \right] \frac{T_s * Z_{avg}}{\eta_{pol}} \left[ \left( \frac{P_d}{P_s} \right)^{\frac{n_{pol}-1}{n_{pol}}} - 1 \right] \left[ = \right] \frac{KJ}{Kg} \quad (3.1.5)$$

$Z_{avg}$  corresponds to the average of the gas compressibility at the suction and discharge conditions and requires gas discharge temperature, with  $Z = Pv/RT$ . The variable  $v$  is the molar volume, i.e. the volume occupied by a mole of gas.  $H_R^{realgas}$  is the effective head required for compressing the real gas and  $H_p^{realgas}$  is the polytropic head required to compress the gas [9].

The equation that follows gives the gas discharge temperature for a polytropic process (being it a function of the pressure ratio) [9]:

$$\frac{Z_d * T_d}{Z_i * T_s} = \left(\frac{P_d}{P_s}\right)^{\frac{n_{pol}-1}{n_{pol}}} \quad (3.1.6)$$

Assuming  $Z_d \approx Z_i$ , we get:

$$\frac{T_d}{T_s} = \left(\frac{P_d}{P_s}\right)^{\frac{n_{pol}-1}{n_{pol}}} \quad (3.1.7)$$

The polytropic exponent ( $n_{pol}$ ) can be obtained from:

$$n_{pol} = \frac{\ln\left(\frac{P_d}{P_s}\right)}{\ln\left(\frac{v_s}{v_d}\right)} = \frac{\ln\left(\frac{P_d}{P_s}\right)}{\ln\left(\frac{Z_i T_s P_d}{Z_d T_d P_s}\right)} \quad (3.1.8)$$

Work is a path-dependent function, meaning that its value depends on the compression path (defined by the polytropic exponent  $n$ ) as well as the start and finish points. Variations in the polytropic exponent  $n$  could alter the value of the calculated work in a typical compression path [9].

The polytropic exponent varies with the pressure and temperature of the gas and compression work calculations need to account for changes in the value of  $n$ . A study on the compression of pure CO<sub>2</sub> found that the polytropic exponent was practically unchanged for pressures less than the critical pressure ( $P_c$ , 73.8 bar) ( $P < P_c$ ) [9].

For values of pressure above the critical one and temperature above 230 °C, the polytropic exponent remains relatively constant. This is not the case when  $P > P_c$  and  $T < 230^\circ\text{C}$ , where it is found that the polytropic exponent varies significantly, between the range of 1.8 and 4 [9].

Since all three regions [i.e.,  $P < P_c$ ;  $P > P_c$ ,  $T < 230^\circ\text{C}$ ;  $P > P_c$ ,  $T > 230^\circ\text{C}$ ] are concerned with intercooled CO<sub>2</sub> compression, it is reasonable to anticipate that work calculations using a constant value of  $n$  would result in inaccurate values. This is particularly true when pressures exceed the critical pressure ( $P > P_c$ ) [9].

### Conventional CO<sub>2</sub> Compression

Isothermal compression of CO<sub>2</sub> at 70 °F (21°C) would produce a crossover to the vapor-liquid zone (see Annex A) before compression to the dense-phase region since the critical temperature of CO<sub>2</sub> is 87.76 °F (31°C) [9].

Additionally, as the volume of the gas changes more in the isentropic scenario, the effort for isentropic compression would be higher than that for isothermal compression. Compressing a gas isothermally is not feasible, though, as actual compression operations invariably involve losses that raise temperature (or entropy) [9].

When comparing the enthalpy of the polytropic and the isentropic processes, there is a sign that for the inlet/discharge pressure and temperature, the work for the isentropic path is lower [9]. Figures 13 and 14 show the possible isentropic and isothermal compression paths on a pressure-

enthalpy diagram and the values for the inlet and discharge pressure as well as the temperature at the compressor for each of the six stages, respectively. [9].

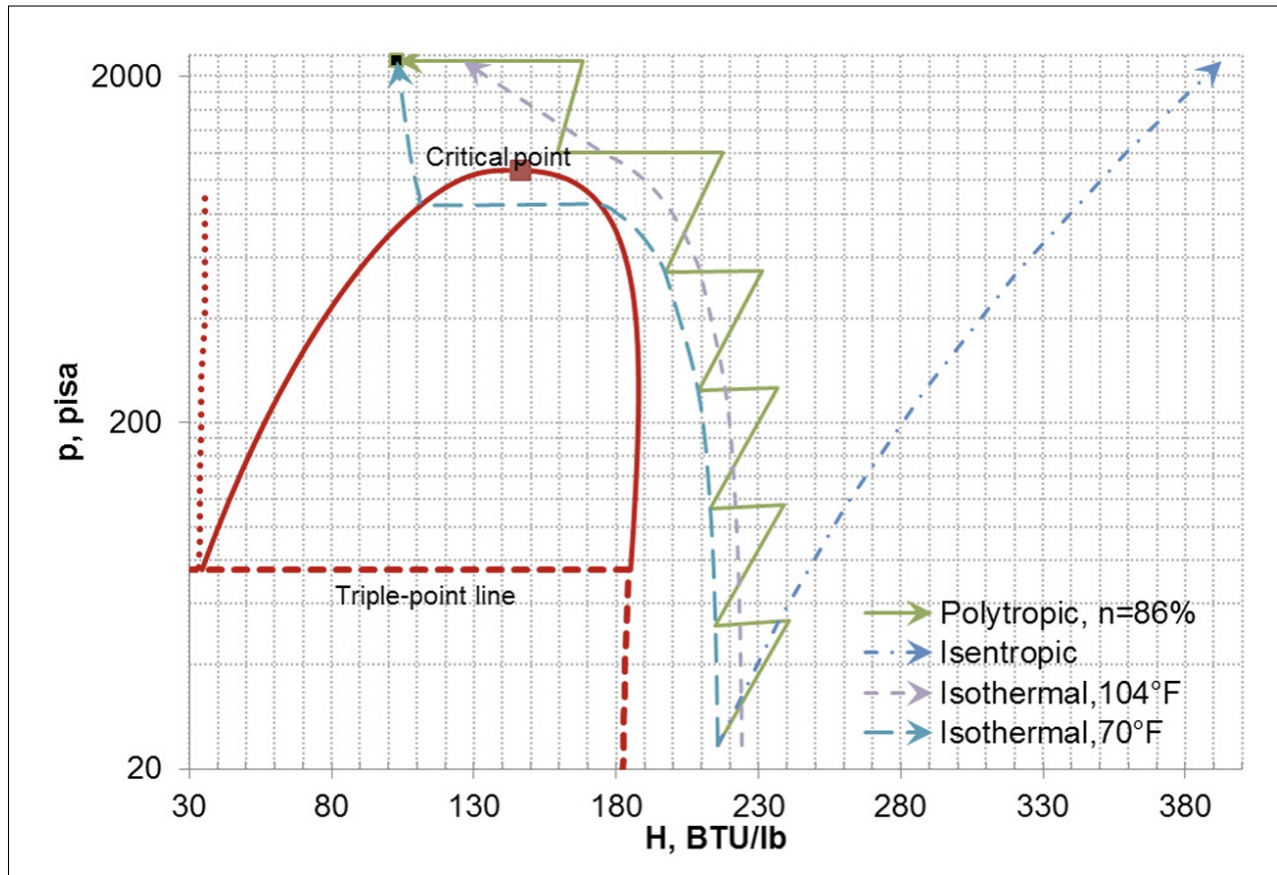


**Figure 13:** Comparison of Isentropic, Isothermal, and Intercooled Polytropic CO<sub>2</sub> Compression ( $\eta_{pol} = 86\%$ ) Paths For compressing CO<sub>2</sub> at 23.5 psia, 70°F (21°C) to 2215 psia., [9].

STAGE	1	2	3	4	5	6
$P_s/P_i$ psia	23.5/53.7	52.0/115.8	113/253	248/550	545/1,205	1,200/2,220
$T_s$ , °F	70.0	70.0	70.0	70.0	70.0	100

**Figure 14:** Inlet and Outlet Pressures for CO<sub>2</sub> Compression Using Conventional Centrifugal Compression with Intercooling Between Stages, [9].

### High-Pressure Ratio Compression

The foundation of high-pressure ratio compressors is shock compression, in which CO<sub>2</sub> is compressed by shock waves produced by a rotor spinning at high (sub-sonic) speeds. Large forces are applied to the compressor shaft when high-pressure ratio compression is used in conventional compressor designs, which results in intricate and expensive designs [9].

The pressure ratio in traditional compressors used in CO<sub>2</sub> compression can only be approximately 2 to 3. Some works have been done on developing a high-pressure ratio shock compression technique that can raise the pressure ratio at each stage from 2 to roughly 10. As a result, the physical dimensions and capital cost of the compressor are lower since the number of stages needed

for compressing to 2215 psia (152.7 bar) is reduced [9].

The integration of compression fluid heat with the SCPC plant's Rankine cycle is another potential benefit of high-pressure ratio compressors. Figure 15 shows a schematic of the high-pressure ratio compression process, in which CO<sub>2</sub> is cooled from the compressor exit temperature to 70 °F (21 °C).

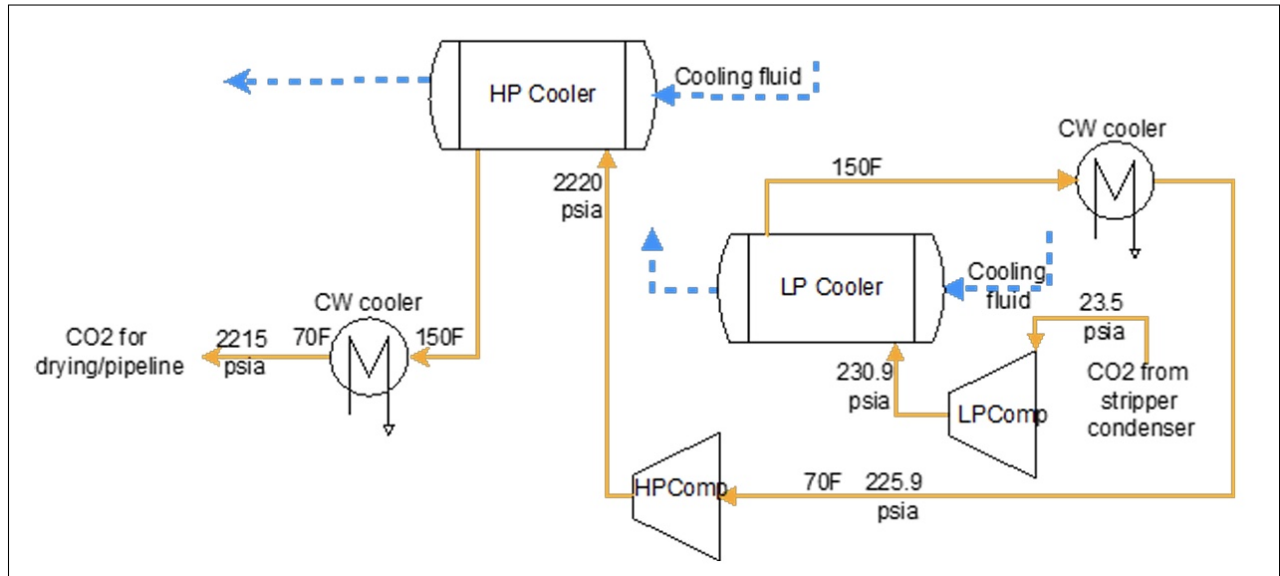


**Figure 15:** Schematic of Two-Stage Compression of CO<sub>2</sub> Using Shock Wave Compression, [9].

In the previous schematic and for performing heat integration at the power plant, the CO<sub>2</sub> would be cooled to 150 °F (65.6 °C) with the help of a cooling fluid followed by a second cooling stage to 70°F (21.1 °C) using cooling water.

Figure 16 represents a comparison between the high-pressure ratio and conventional compression paths on a pressure-enthalpy diagram. Results shown in Table 4-1 indicate that the use of an EOS-based integration approach (Prode), or Schultz polytropic procedure with a high-fidelity EOS

The results presented on figure 17 are based on an EOS-based integration approach (Prode) and on the Schultz polytropic procedure for calculating the temperature at the discharge, the head and the compression power, [9].

As it is clear to see, the enthalpy at the compressor stage outlet is much higher for the case of high-pressure ratio compressors when comparing to conventional compressors. Due to the higher values of discharge temperature on the high-pressure ratio compression (446-472 °F in comparison to 167-192 °F in conventional compression), and higher fluid volume to be compressed, the compressor load for high-pressure ratio compression is significantly higher than the conventional compression one (30.16% higher to be more precise) [9].

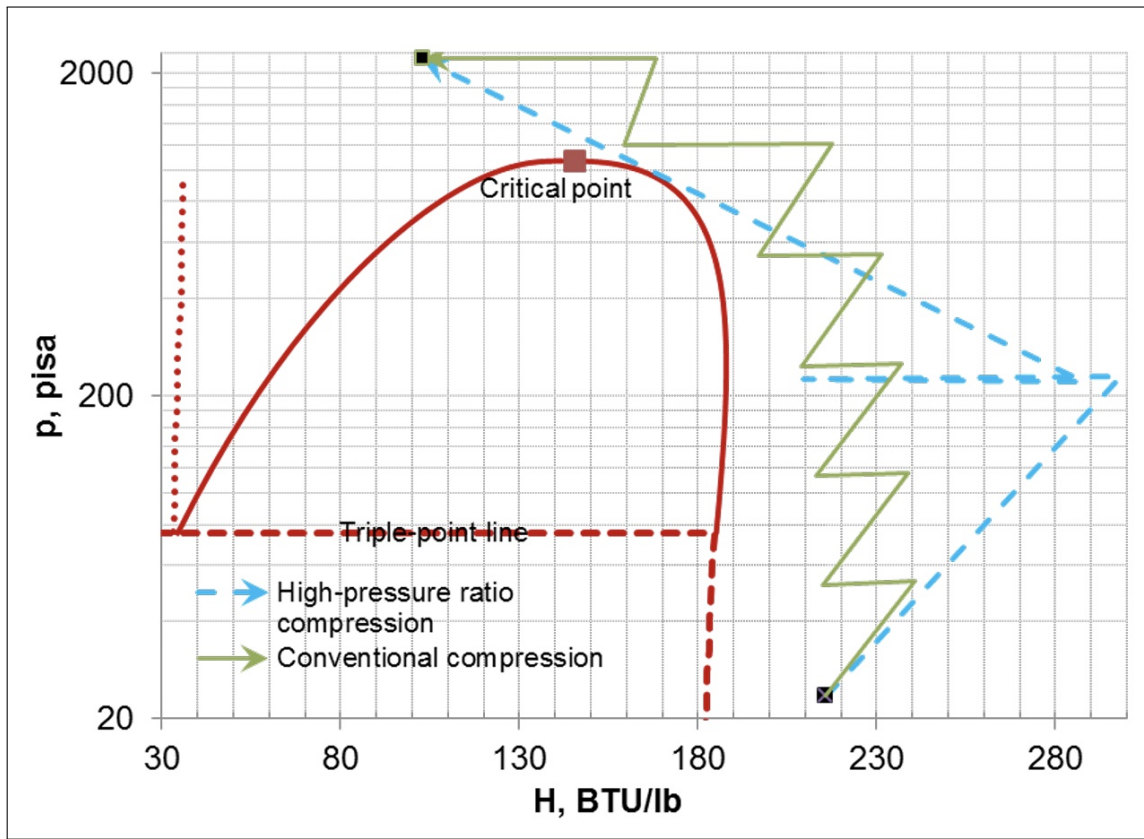


Figure 16: p-H Diagram for Conventional and High-Pressure Ratio CO<sub>2</sub> Compression ( $\eta_p = 86\%$ ), [9].

STAGE	1	2
$P_{sr}$ , psia	23.5	225.9
$T_{sr}$ , °F	70	70
$P_{dr}$ , psia	230.9	2,220.0
Pressure ratio	9.83	9.83
$T_{dr}$ , °F (Prode)	446.8	472.4
$T_{dr}$ , °F (Schultz)	452.4	471.5
Head ( $\Delta h$ ), kJ/kg (Prode)	192.2	182.1
Head ( $\Delta h$ ), kJ/kg (Schultz)	195.5	181.5
Gas power, hp/(lb <sub>m</sub> /min) <sup>11</sup>	3.80	
Total, kWe (Prode)	58,199	
Total kWe (Schultz)	58,613	

Figure 17: Stage Outlet Temperature, Head, and Overall Compression Load for the Two-Stage Compression of CO<sub>2</sub> from 23.5–2,215 psia using Prode and Schultz calculations, [9].

## Isothermal CO<sub>2</sub> Compression/Cooled-Diaphragm Concept

When a fluid is compressed isothermally, its temperature doesn't change. The heat generated during compression must be expelled as soon as it is created in order for isothermal compression to occur. Using external intercoolers to cool the gas between compression stages is the traditional method of reducing temperature [9].

With external intercooling, it is possible to get almost isothermal operation with multi-shaft, integral-gear centrifugal compressors. Besides that, their reliability is lower in contrast to single-shaft in-line centrifugal compressors, which also provide more operational flexibility[9].

Instead of utilizing interstage cooling, the Southwest Research Institute (SwRI) is creating a method that uses an internal jacket to continuously cool CO<sub>2</sub> in the compressor diaphragm. Research indicates that the cooled-diaphragm approach can reduce the compression load by 6 to 12%. The cooled-diaphragm technology performs similarly to isothermal compression [9].

Prior research by SwRI indicates that compared to a compression method with gas cooling, a low-pressure compression approach utilising a cooled diaphragm, liquefaction, and pumping uses more energy [9].

## 3.2 CO<sub>2</sub> transport

One of the most important parts of carbon capture, transportation, storage, and monitoring is CO<sub>2</sub> transportation. To find the most cost-effective transportation option, the complete process from the CO<sub>2</sub> source to the storage facility must be taken into account, as seen in Fig. 18 [12].

Prior to CO<sub>2</sub> pipeline transport, compression and other impurity removal processes (such as dehydration) are frequently necessary once the CO<sub>2</sub> has been captured. Different CO<sub>2</sub> processing techniques, such as dehydration, chilling, liquefaction, distillation, temporary storage at the source and destination, and pumping, are needed for liquid CO<sub>2</sub> transport [12].

The project's size, duration, distance, and the circumstances and methods used for CO<sub>2</sub> capture and transport are important factors in CO<sub>2</sub> transport. Pipelines are the main large-scale transport mechanism for CO<sub>2</sub>, although there are other options as well. CO<sub>2</sub> transport through pipeline is performed in a homogeneous phase characterised by high density and low viscosity, making it the most cost effective method for CO<sub>2</sub> transportation. On this type of transport, CO<sub>2</sub> is compressed above its critical pressure, typically to a minimum of 83 bar [12].

CO<sub>2</sub> can also be transported in trucks, railcars, and ships as a liquid at low temperatures (−18 °C) and relatively low pressures ( 20 bar). These alternative techniques are usually more cost-effective across shorter distances and smaller scales. In order to enhance liquid CO<sub>2</sub> density and vessel transport capacity, larger ship transport sizes and quantities that are being considered for future projects may carry the liquid at lower temperatures and pressures that are nearing the CO<sub>2</sub> triple point (−56.6 °C, 5.2 bar). In the future, larger ships might be preferable to pipelines for certain projects, based on the volume, distance, and other particulars of the project. [12].

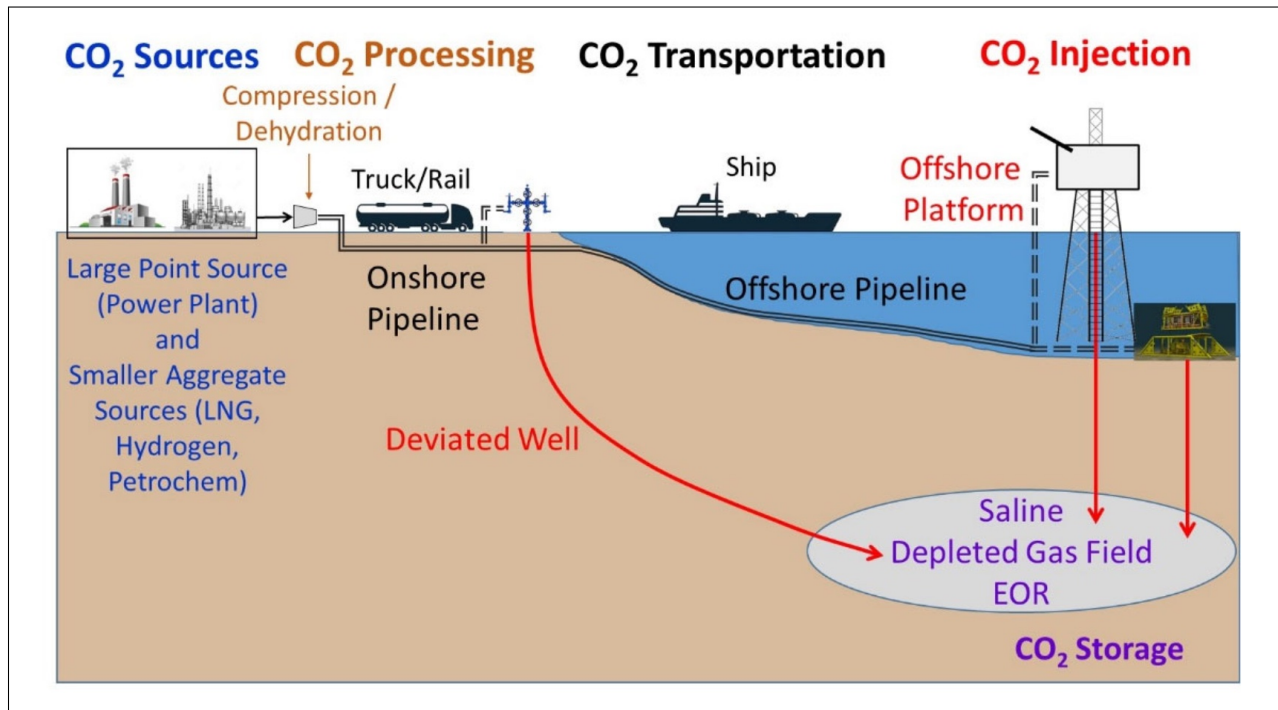


Figure 18: Example CO<sub>2</sub> source and transportation options, [12].

There are many feasible means for transporting CO<sub>2</sub> which include pipeline, ship, truck and rail. All of these transport methods will be discussed on the following sections.

### 3.2.1 Ship Transport

For some regions, ship transportation can be a cost-effective way to transfer CO<sub>2</sub>. In areas with numerous waterways and dispersed point sources, ships could be utilised to transport CO<sub>2</sub>. For transcontinental or intercontinental CO<sub>2</sub> transmission, shipping might also be more economical than building new, drawn-out pipes [12].

The CO<sub>2</sub> is transported as a liquid at low temperatures in order to maintain high density CO<sub>2</sub> and reduce the size and pressure rating required of the ship. At  $-28^{\circ}\text{C}$  and a pressure of about 15 bar, the CO<sub>2</sub> is transported. In comparison to pipeline transport, this necessitates more thorough dehydration. It also calls for refrigeration, CO<sub>2</sub> condensation (liquefaction), pumping procedures, and frequently distillation to get rid of contaminants including oxygen, nitrogen, and methane. This method also usually calls for temporary liquid CO<sub>2</sub> storage (capacity for one to three days storage of the average daily transport rate) at both the source and storage location because the CO<sub>2</sub> transport will take place in sporadic batch shipments [12].

### 3.2.2 Truck Transport

A dependable and adaptable way to move CO<sub>2</sub> on a small scale is with a truck. CO<sub>2</sub> is frequently transported by truck for industrial, food, and beverage applications. Although truck sizes vary from 2 to 30 tonnes, a typical vehicle can carry up to 18 tonnes of liquid CO<sub>2</sub> [12].

For economic reasons, the distance between the CO<sub>2</sub> collecting facility (source) and the storage location (destination) is typically restricted to approximately 320 kilometres. Usually, the CO<sub>2</sub> liquid is carried at a temperature of  $-23^{\circ}\text{C}$  and roughly 18 bar. To help with temperature regulation and to cut down on evaporative losses, the trucks are insulated. About 1% of CO<sub>2</sub> is released from the vehicle during loading and unloading thanks to vapour balancing on both the truck and the loading/receiving vessel [12].

Figure 20 shows a transport truck for refrigerated liquids such as CO<sub>2</sub> (on the left-side) and a portable liquid CO<sub>2</sub> storage trailer on the right side.

Trucks can help move small amounts of CO<sub>2</sub> between ports and industrial locations, which can help with ship transportation. In places where pipelines or ship transportation are not yet feasible, trucks can also move CO<sub>2</sub>. A single CO<sub>2</sub> delivery truck may be purchased for roughly 290,000 USD. Operating costs comprise things like fuel, maintenance and repairs, insurance, licences, and other items, as well as labour to operate the trucks and discharge the CO<sub>2</sub> [12].



**Figure 19:** Transport truck for refrigerated liquid (left-side) and portable liquid CO<sub>2</sub> storage container (right-side), [12].

### 3.2.3 Rail Transport

Rail transport stands as a beacon of efficiency and environmental responsibility, offering a robust solution for the movement of CO<sub>2</sub> across vast distances with reduced carbon footprint, despite the higher evaporative and loading losses that it presents.

In fact, an introductory load of 80 tonnes in a rail car might result in a net delivery of only 63 tonnes, depending on rail travel time and loading / unloading operations. Travel times can be expanded essentially on the off chance that the devoted track isn't accessible between source and destination. Rail cars containing CO<sub>2</sub> can hold up sit still for numerous days until the track is accessible once more. Rail cars are prepared with three types of pressure relief devices, and standard venting of vapor is normal to decrease internal pressure. Ordinary transport losses of CO<sub>2</sub> extend from 9% to 16% [12].

Empty rail cars are initially transported via rail to the originating facility. Subsequently, these cars are filled from CO<sub>2</sub> storage tanks at the source facility with liquid CO<sub>2</sub>, typically maintained at approximately 15 bar and  $-28^{\circ}\text{C}$ . Each car is equipped with approximately 127 mm of urethane foam insulation to sustain CO<sub>2</sub> temperatures during the 8-10 day transit period. Following loading, the

rail car is conveyed from the loading facility to the unloading facility by a rail freight service provider. At the unloading facility, the rail cars are emptied and then transported back to the loading facility by the same freight company. Loading and unloading of rail cars require a significant amount of time due to the necessity of connecting/disconnecting the rail cars at the loading platform and maneuvering them into position [12].

Railway cars are employed to transport CO<sub>2</sub> typically covering distances of up to 1610 km. According to an industry expert, a general guideline suggests that truck transportation tends to be more cost-effective than rail transportation for distances spanning up to 640 km. Hence, it's plausible that the most advantageous range for rail transportation falls between 640 km and 1,610 km [12].

Additionally, more transportation volume may favor rail to trucking. Point-to-point rail cars have the potential to serve as a temporary transport solution on CCUS projects until other transport options, such high-capacity transport ships or pipelines, are constructed. A single rail car costs roughly 230,000 USD. Rail yard expenses and a railcar moving device to move rail cars around the switching yard could be additional capital expenses. Shipping and labour costs for loading and unloading rail carriages are included in operating expenditures [12].

### 3.2.4 Pipeline Transport

The most cost-effective method for moving large volumes of carbon dioxide (CO<sub>2</sub>) across long distances is pipeline transportation, out of all the available methods [11].

Research has been done on both supercritical and dense phase CO<sub>2</sub> pressure drop behaviour in pipeline transportation and it has been concluded that the pressure along the pipeline keeps dropping until CO<sub>2</sub> evaporates and the pipeline may eventually be blocked, confirming the need for the definition of a maximum safe transport distance. In case CO<sub>2</sub> transportation needs to extend beyond this maximum distance, additional pump stations should be installed along the pipeline [11].

CO<sub>2</sub> can be carried in two different states over long distances: subcooled liquid or supercritical fluid. Because of the high pressure drop and low density, gas-phase transport has drawbacks. Transporting CO<sub>2</sub> in a subcooled liquid state generally has some advantages over transporting it in a supercritical state. This is primarily due to the liquid's higher density and lower compressibility within the pressure range under consideration, which allows for smaller pipe sizes and reduces pressure losses [11].

Depending on the pressure and temperature within the pipeline system, CO<sub>2</sub> can technically be transported through pipes as a gas, a supercritical fluid, or a subcooled liquid [11].

Being CO<sub>2</sub> a very corrosive medium, it is necessary to lower the water content to less than 60% of the saturation stage. Condensation removes some of the moisture in the intercooled compression scenario. After the last compressor step, however, there is still a need to supply an additional drying stage [11].

Besides that, the variation of carbon dioxide compressibility with pressure must be taken into account, making sure that all the transport process is performed within the recommended region

(see appendix A).

Typically, the pipelines used for the transport of CO<sub>2</sub> are buried at least 1 m underground. When existing infrastructure prevent underground installation of CO<sub>2</sub> pipelines, there is the need for the usage of aboveground CO<sub>2</sub> transmission pipelines (see Figure 19). As demonstrated, because hourly and seasonal fluctuations in weather can have a major impact on the CO<sub>2</sub> density in the aboveground pipeline, insulation may be necessary on aboveground pipes in order to maintain stable injection temperature and pressure throughout the year [12].



**Figure 20:** 400 mm diameter commercial CO<sub>2</sub> pipeline at above/below ground transition, [12].

CO<sub>2</sub> pipelines can be installed onshore or offshore. Onshore pipelines for CO<sub>2</sub> can be constructed similarly to pipelines for natural gas transmission. Routing, topography, the quantity of roads and river crossings, pipe hydraulics and material quality/thickness, internal and external corrosion protection, the necessity of booster compression (or pumping), rights of way, and pigging are a few of the crucial factors that must be taken into account during the design process [12].

Building offshore CO<sub>2</sub> pipes may be similar to building offshore hydrocarbon pipelines if the CO<sub>2</sub> is non-corrosive (dehydrated to prevent any liquid water from developing in the CO<sub>2</sub>). The pipeline's path along the seabed, pipe hydraulics, material/quality thickness, stability of the pipeline on the seabed, external corrosion protection, influence from outside parties, and installation technique are a few of the crucial design criteria [12].

The use of natural gas pipes for CO<sub>2</sub> transportation will probably only be permitted in certain circumstances involving shorter distances and more constrained transport capacity. This is because the pressure at which CO<sub>2</sub> is normally transported is higher than that of natural gas, therefore CO<sub>2</sub> requires a pipeline with a higher pressure rating (ANSI 900, or 153 bar), compared to ANSI 600, or 102 bar, for natural gas) [12].

Transporting CO<sub>2</sub> would require a lot more booster stations if the pipeline was solely designed for natural gas pressure. This would result in a large rise in the capital and operating costs of CO<sub>2</sub> transportation, especially when transport quantities and distances increase. Daily operations, maintenance and inspections, and environmental and safety-related tasks are all part of pipeline operational maintenance. Transport losses of CO<sub>2</sub> in pipelines are typically very small [12].

### Methodology for Pipe Design

Numerous factors come into play when designing a pipeline. Pipeline pressure is determined by hydraulic considerations such as pressure drop, elevation changes, and the pressure needed at the injection well, occasionally influenced by density requirements at booster stations. The initial temperature of the pipeline is usually determined by the available cooling medium at the source (e.g., cooling water or air cooling). Heat exchange with the surroundings leads to the CO<sub>2</sub> temperature stabilizing at a consistent level within the underground pipeline, which can vary depending on location and other factors, with 30°C being a common value. Furthermore, the presence of impurities in the CO<sub>2</sub> sources entering the pipeline must also be taken into account [12].

Most CO<sub>2</sub> sources, including those from common CO<sub>2</sub> capture processes, are typically saturated with water vapor. Upon subsequent cooling, this can lead to the formation of a free (liquid) water phase through condensation. Carbon steel, commonly used in pipelines, is susceptible to corrosion in the presence of free water and CO<sub>2</sub> [12].

While some water is naturally removed during CO<sub>2</sub> compression and cooling, this may not be enough to prevent the risk of water condensation or free water formation within carbon steel pipelines. Therefore, additional dehydration of CO<sub>2</sub> is typically required to mitigate this risk during operation, shut-in periods, and extreme weather conditions. One prevalent method for water removal is through a triethylene glycol (TEG) absorption unit, although alternative methods exist. This dehydration unit is typically integrated into the compression train at an intermediate pressure (usually around 45 bar), where the water content of CO<sub>2</sub> is naturally minimized due to prior compression and cooling stages. This integration helps to reduce both the capital and operating costs associated with the dehydration process [12].

Oxygen removal may be necessary, particularly when transporting CO<sub>2</sub> via common carrier pipelines or for enhanced oil recovery (EOR) purposes. When CO<sub>2</sub> containing oxygen comes into contact with a free liquid water phase, the resulting mixture becomes significantly more corrosive compared to oxygen-free CO<sub>2</sub>. Similarly, the removal of H<sub>2</sub>S is often warranted due to concerns regarding toxicity, corrosion, and stress cracking in certain steel grades [12].

Additionally, non-condensable gases like hydrogen (H<sub>2</sub>), methane (CH<sub>4</sub>), and nitrogen (N<sub>2</sub>) present in the CO<sub>2</sub> stream at pipeline conditions can reduce pipeline capacity, increase compressor/pump power requirements, and impair the CO<sub>2</sub> mixture's suitability for EOR applications. The type and quantity of impurities in the CO<sub>2</sub> stream vary depending on the emission source and the processes employed for capturing, compressing/pumping, and dehydrating the CO<sub>2</sub>. Table 2 provides example specifications for some existing pipelines [12].

Key factors in calculating pipeline flow capacity include the internal diameter, fluid density and viscosity, pipeline length, pressure drop along the pipeline, terrain profile, and the temperatures of both the surroundings and the fluid, [13].

**Table 2:** Existing Pipeline Specifications, [12].

Component	Units	Limit Ranges
CO2 purity	% vol.	$\geq 95$
H2O	ppmv	$< 250-950$
H2S	ppmw	$< 10-45$
N2	%vol.	$< 0.9$ to 4
O2	ppmv	$< 10$
Hydrocarbons	% vol.	$< 4-5$
Glycol	ppbv	$< 46$
Temperature	$^{\circ}\text{C}$	$< 32.2$ to 48.9
Pressure	bar	$\geq 83.7$ and $\leq 152.7$

### Diameter Calculation

An initial estimation for the value of the pipe diameter can be attained through the equation of the velocity,  $v$ , of CO<sub>2</sub> in the pipeline. According to the International Energy Agency Green-house Gas R and D Programme, [14], a recommended value for the velocity is 2 [m/s] and can be used as a base reference.

The equation that allows for the computation of the velocity,  $v$ , is the one that follows:

$$v = \frac{P_b}{T_b} * \frac{Z * T_f}{P_{in}} * \frac{Q_b}{\pi D^2} * \frac{4}{24 * 3600} \quad (3.2.1)$$

The standard volume flow rate,  $Q_b$ , is in  $m^3/day$  at base temperature,  $T_b$ , and base pressure,  $P_b$  (at STP);  $T_f$  is the flow temperature of CO<sub>2</sub>;  $P_{in}$  is the inlet pressure and  $Z$  is the compressibility factor. The standard mass flow rate can be calculated from the capacity of the pipeline as:

$$Q_b = \frac{m_{CO_2}}{\rho_b} \quad (3.2.2)$$

Where  $m_{CO_2}$  is the mass flow in the pipeline in t/day and  $\rho_b$  is the density of CO<sub>2</sub> at base temperature and base pressure.

### Calculation of Wall Thickness

The necessary pipe wall thickness for pipeline transport is described in national standards. Due to the fact that CO<sub>2</sub> is transported at higher pressures than natural gas, CO<sub>2</sub> pipelines should present greater wall thickness. The pipe wall thickness recommended can be attained by the fol-

lowing equation, [14]:

$$t = \frac{P_{max}D}{2(S * F * E - P_{max})} \quad (3.2.3)$$

On the previous equation,  $P_{max}$  is the design pressure, i.e. the maximum valuable for the pressure inside the pipeline.

### Pressure Drop Calculation

To calculate the pressure drop,  $\Delta P$ , along the length of the pipeline, the Darcy-Weisbach equation is applied. The pressure drop is then computed by the following equation:

$$\Delta P = f * \frac{L}{D} * \rho * \frac{v^2}{2} \quad (3.2.4)$$

### Pressure Boosting

Pressure boosting is required to re-pressurize the CO<sub>2</sub> stream, compensating for pressure losses and ensuring the stream remains in a dense phase. This is essential to prevent a two-phase flow condition. The booster station should be positioned where the pressure is expected to approach the two-phase boundary, as determined by design conditions. Comprehensive hydraulic gradient studies are needed to identify the necessary number of boosting stations. While initial compression levels can be increased to extend the distance before boosting is required, this is constrained by the pipeline's pressure rating, [13].

### 3.2.5 Comparison of Characteristics for CO<sub>2</sub> Transport Methods

Table 3 presents a comparison of essential features for various CO<sub>2</sub> transportation methods, including the CO<sub>2</sub> transport stage, typical operating conditions, approximate maximum capacity, and broad cost differentials. The cost figures in the table are broad and offer a basic overview of the comparative economic aspects of the diverse transport alternatives. It is important to note that CO<sub>2</sub> transport expenses should be evaluated individually for each project, considering specific requirements, applications, and operational circumstances. Mt, t and y stand for million tonne, tonne and year, respectively, [12].

The costs associated to impurity removal (e.g., dehydration) and CO<sub>2</sub> compression to the supercritical phase were not included on table 2. For a typical 1 000 000 t/y plant capacity, this additional costs are in the order of 15 USD / tonne. The additional costs for dehydration, liquefaction and compression of CO<sub>2</sub> to 150 bar are on the order of 19 USD / tonne, again for a typical 1 000 000 tonne/year plant capacity. For reference, the purchase cost of liquid CO<sub>2</sub> at ship, rail or truck transport conditions are approximately 66 USD/tonne [12].

The expenses associated with CO<sub>2</sub> pipelines can fluctuate significantly based on several factors such as location (including environmentally or culturally sensitive regions, rural versus urban areas, and rugged terrain), material costs, and operational conditions (such as capacity, distance, temper-

**Table 3:** Key characteristics for CO<sub>2</sub> transport methods, [12].

CO <sub>2</sub> Transport Method	Typical CO <sub>2</sub> Transport Phase And Operating Conditions	Estimated Maximum Capacity	Generalized Cost of CO <sub>2</sub> Transport
Pipeline (on-shore)	Supercritical/dense phase (130 bar and 30°C)	52 600 t / day (19.3 Mt/y)	7 €/ t per 100 km  (for > 10 Mt / y)
Pipeline (off-shore)	Supercritical/dense phase (130 bar and 21°C)	52 600 t / day (19.3 Mt / y)	14 € / t per 100 km  (for > 10 Mt / y)
Ship (marine)	Saturated liquid (15 bar and -28°C) or at (8 bar and -50°C)	45 000 t / vessel	62 € / t per 7 600 km  each trip for using 17 tankers  (20 000 t / each) 5.5 Mt / y
Rail	Saturated liquid (15 bar and -28°C)	70t/railcar	110 €/t
Truck	Saturated liquid (15 bar and -28°C)	18 t/tanker	110 €/t

ature, and pressure). For instance, installing a pipeline in a remote region may cost roughly three times less (approximately 1679 USD per kilometer of pipeline per pipeline diameter in millimeters) compared to constructing a pipeline in a densely populated industrial or suburban area near a major city (costing around 4873 USD per diameter millimeter-kilometer). The costs associated with offshore pipelines are higher due to the specialized equipment needed for constructing pipelines underwater. Offshore pipelines can be approximately twice as expensive as their onshore counterparts [12].

Transport by ship may be more economical than by pipeline for distances higher than 1000 km and CO<sub>2</sub> flow of less than a few million tonnes per year.

The cost of ship transport was derived from a figure found in literature describing a marine transport system capable of carrying 5.5 million tonnes per year. This system comprises 17 tankers, each with a capacity of 20 000 tonnes, traveling 7600 kilometers per trip at a speed of 35 kilometers per hour. The transport cost was estimated at 34 USD per tonne [12].

The choice of CO<sub>2</sub> transport method for a particular project should be made following an evaluation of both the upstream carbon capture process and system, as well as the downstream injection and storage conditions, in order to achieve the most efficient overall design for the CCS or CCUS project. Additionally, the locations of the CO<sub>2</sub> sources and injection wells (whether they are inland, onshore near waterways, or offshore) will also influence the selection of the CO<sub>2</sub> transport method [12].

### 3.3 Economics of $CO_2$ Compression and Transport

The following section presents a detailed cost analysis for the acquisition and operations and maintenance of a generic pipeline infrastructure.

#### 3.3.1 Pipeline Costs

The pipeline's associated costs can be separated into two categories: investment costs and operating costs. The diversity of topography conditions makes it difficult to predict the investment costs associated with pipeline projects.

Many studies have attempted to estimate these costs using data that is accessible to the public. An approximation of 40 euros per metre of pipeline length per inch of diameter (€/inch/m) is the investment cost assumption based on these investigations. The cost employed in this research's computations is a generalisation for pipes made of carbon steel. Then, for various pipeline diameters, this cost value (2010) is scaled to the present market (2024), [15].

The investment cost of the pipeline length per meter,  $IC_{pipe}$ , is then given as:

$$IC_{pipe} = 40 * D / 0.0254 * (1 + I_{cum}) \quad (3.3.1)$$

With  $I_{cum}$  being the cumulative inflation rate of € from 2010 to 2024.

The total investment cost of the pipeline,  $Invest_{pipe}$  can be calculated as:

$$Invest_{pipe} = IC_{pipe} * L \quad (3.3.2)$$

The pipeline's operations and maintenance (O&M) expenses are determined as a percentage of the investment cost. It suggests that more frequent maintenance is needed for pipeline projects that are bigger and more intricate. A yearly fixed O&M factor of 2.6% has been established in this study based on the following: 1% each for insurance and property taxes, 0.5% for maintenance and repairs, and 0.1% for licensing and permits, [15].

The pipeline's O&M expenses can be computed as:

$$O\&M_{pipe} = 0.026 Invest_{pipe} \quad (3.3.3)$$

The levelized cost of carbon dioxide transport (LCO2T) for pipeline investment  $LCO2T_{pipe,Invest}$  can be calculated as:

$$LCO2T_{pipe,Invest} = \frac{Invest_{pipe} * CRF_{pipe}}{CF_{pipe} * mCO2,year} \quad (3.3.4)$$

Where  $CRF_{pipe}$  is the capital recovery factor of the pipeline;  $CF_{pipe}$  is the capacity factor of the pipeline which indicates the amount of time in a year in which the pipeline can operate effectively; and  $m_{CO_2,year}$  in t/year is the total capacity of the pipeline or the amount of  $CO_2$  transported in a year, [15].

The capital recovery factor can be calculated with the interest rate,  $i$ , and the lifetime,  $n$ , as:

$$CRF = \frac{i * (1 + i)^n}{(1 + i)^n - 1} \quad (3.3.5)$$

The LCO2T for pipeline O&M costs  $LCO2T_{pipe,O\&M}$  and the total LCO2T for the pipeline  $LCO2T_{pipe}$  can be calculated as:

$$LCO2T_{pipe,O\&M} = \frac{O\&M_{pipe}}{CF_{pipe} * m_{CO_2,year}} \quad (3.3.6)$$

$$LCO2T_{pipe} = LCO2T_{pipe,Invest} + LCO2T_{pipe,O\&M} \quad (3.3.7)$$

### 3.3.2 Compressor and Pump Costs

$CO_2$  is first present in the gaseous phase following the initial capture. After processing, it passes via a compressor, reaching 73.8 bar, the critical pressure. The critical point is a thermodynamic condition in which  $CO_2$  does not exist as separate liquid and gas phases, but rather as a supercritical fluid with characteristics of both phases. The pressure is then increased to the inlet value,  $P_{in}$  by a pump, which causes the phase to become dense. Because of its high density and low viscosity, this dense phase is perfect for pipeline transfer, [15].

$CO_2$  transportation, as any other fluid, has transportation losses caused by friction, elevation, and temperature difference, which results on pressure loss. If the  $CO_2$  pressure during the transport achieves a value close to the phase transition point, it is necessary to add a booster station which is responsible for the repressurize of the  $CO_2$ . Finally, the  $CO_2$  arrives at its destination, where it can be used in different applications, [15].

This could include subterranean storage, use in enhanced oil recovery, industrial uses, or even carbonation procedures used in the food and beverage sector. The sequential procedures involved in the transportation and utilisation of  $CO_2$  are depicted in the block diagram in Figure 20.

For the computation of the required compressor power in order to reach the  $CO_2$  critical pressure, the following equation may be used, [15]:

$$W_{s,i} = \frac{1000}{24 * 3600} * \frac{mZ_sRT_{in,comp}}{M\eta_{is}} * \frac{k_s}{k_s - 1} (CR^{\frac{k_s-1}{k_s}} - 1) \quad (3.3.8)$$

On the previous equation,  $m$  is the mass flow rate of  $CO_2$  in t/day,  $Z_s$  is the average  $CO_2$  compressibility factor for each compression stage;  $R$  is the universal gas constant;  $M$  is the molecular

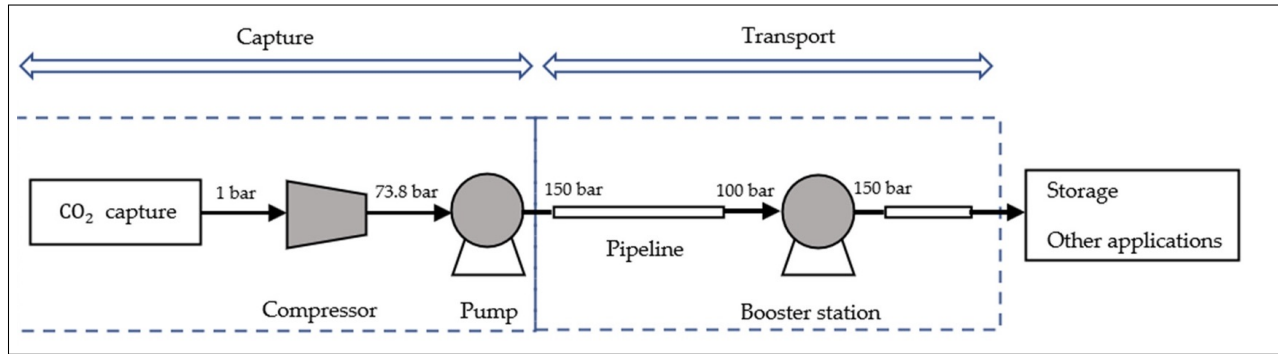


Figure 21: CO<sub>2</sub> processing block diagram, [15].

weight of  $CO_2$ ;  $T_{in,comp}$  is the temperature of  $CO_2$  at the compressor inlet;  $\eta_{is}$  is the isentropic efficiency of the compressor;  $W_{s,i}$  is the compression power requirement for each stage in KW and  $k_s$  is the average ratio of specific heats of  $CO_2$  for each stage and is given by:

$$k_s = \frac{C_p}{C_v} \quad (3.3.9)$$

For the computation of the specific heat at constant pressure,  $C_p$ , and the specific heat at constant volume,  $C_v$ , it can be used the values of the average pressure of the pressure range and average temperature of each compression stage. Because intercooling continuously lowers the temperature to the same level and maintains steady pressure ratios throughout, the average temperature stays constant. As a result of polytropic compression, the maximum temperature is likewise constant across all phases. Moreover, this is how the compression ratio (CR) is computed, [15]:

$$CR = \left( \frac{P_{cut-off}}{P_{initial}} \right)^{\frac{1}{N_{stage}}} \quad (3.3.10)$$

$P_{cut-off}$  is the outlet pressure of the compressor, in this case the  $CO_2$  critical pressure, and  $P_{initial}$  is the inlet pressure of the compressor, in this case, the  $CO_2$  pressure after capture.

It was considered a total of 5 compression stages for allowing consistent temperature control through intercooling, enhancing the overall efficiency of the compression process. The following equation shows how the total compression power,  $W_{comp}$  can be computed, in KW, considering the power in each compression stage,  $W_{s,i}$ :

$$W_{comp} = \sum_{i=1}^5 W_{s,i} \quad (3.3.11)$$

Figure 21 that follows represents a  $CO_2$  phase diagram where it was included an orange rectangle corresponding to the range at which dense phase  $CO_2$  transport is typically performed.

After  $CO_2$  compression up to its critical pressure, a pump is necessary for achieving the final pressure for pipeline inlet,  $P_{final}$  which will allow for  $CO_2$  transportation at the dense phase region.

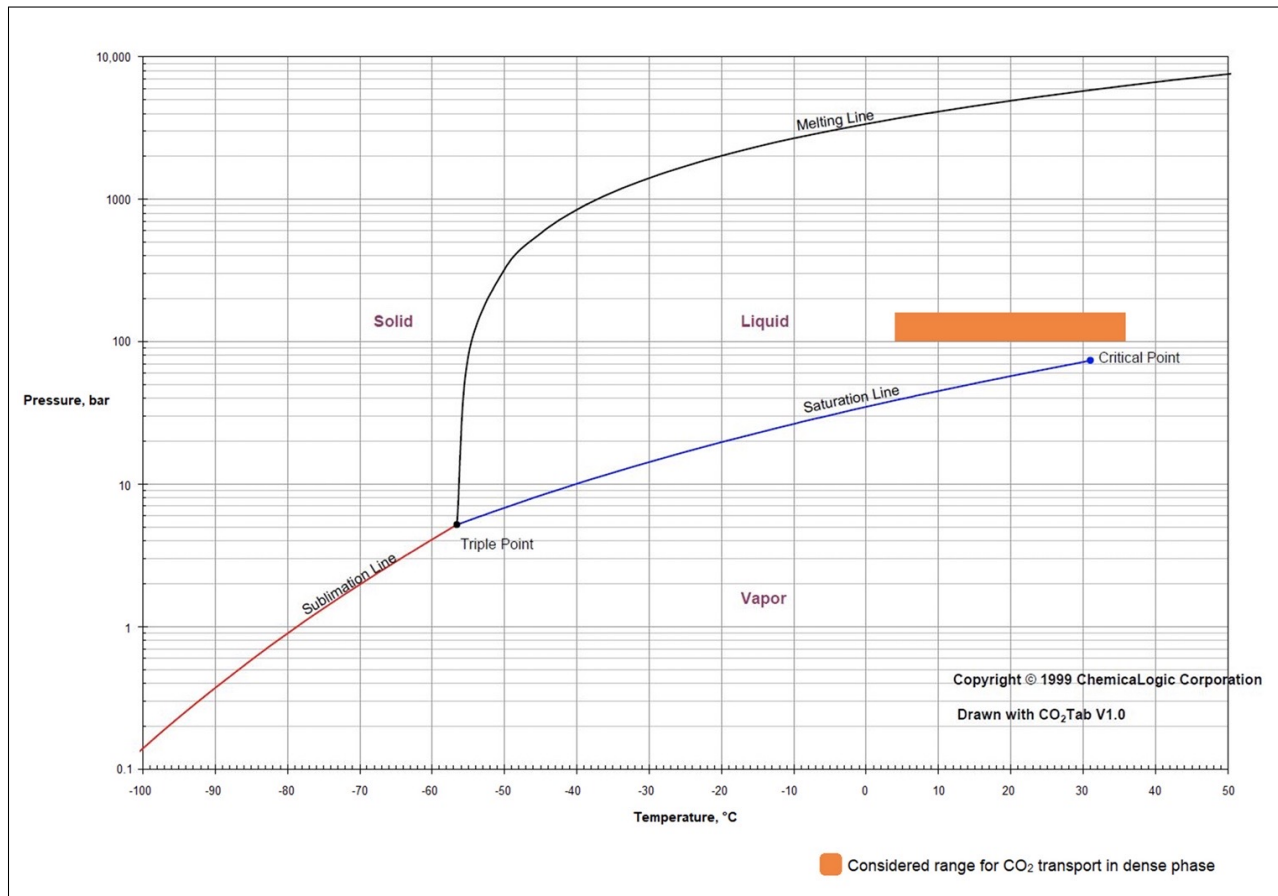


Figure 22:  $CO_2$  phase diagram, [15].

The equation that follow shows the way of computing the necessary pumping power,  $W_{pump}$ , in KW.

$$W_{pump} = \frac{1000}{24 * 36} * \frac{m(P_{final} - P_{cut-off})}{\rho \eta_p} \quad (3.3.12)$$

On the previous equation,  $\eta_p$  is the pump efficiency,  $\rho$  is the density of  $CO_2$  at the average pressure and inlet temperature during pumping. For this, it was assumed that the temperature rise of  $CO_2$  during pumping is negligible compared to compression, [15].

The costs associated to compression,  $C_{comp}$ , in M€ are computed as:

$$C_{comp} = C_{0,comp} \left( \frac{W_{comp}}{W_0} \right)^{y_{comp}} * N_{train,comp}^{me} * (1 + I_{cum}) \quad (3.3.13)$$

This cost includes aftercooling to about 30°C.  $C_{0,comp}$  is the base cost (2010) of the compressor;  $W_0$  is the base scale of the compressor;  $W_{comp}$  is the compression power per unit;  $y_{comp}$  is the compressor scaling factor;  $me$  is the multiplication exponent;  $I_{cum}$  is the cumulative inflation rate of € from 2010 to 2024 and  $N_{train,comp}$  is the number of parallel compressor units, which is calculated

as, [15]:

$$N_{train,comp} = Roundup\left(\frac{W_{comp}}{W_{comp,max}}\right) \quad (3.3.14)$$

Where  $W_{comp,max}$  is the maximum capacity of a compressor unit.

For the costs associated to the  $CO_2$  pump, the literature assumed a similar pump design to water pumps in estimating costs, since  $CO_2$  is to be used at the liquid phase. The following equation gives the cost model for  $CO_2$  pumps, [15]:

$$C_{pump} = C_{0,pump} * W_{pump}^{y_{pump}} * N_{train,pump}^{me} * (1 + I_{cum}) \quad (3.3.15)$$

The total pump investment cost,  $C_{pump}$ , is in k€;  $C_{0,pump}$  is the base cost of the pump;  $y_{pump}$  is the pump scaling factor;  $W_{pump}$  is the pumping power per unit in KW; me is the multiplication exponent and  $N_{train,pump}$  is the number of parallel pump units and is given by:

$$N_{train,pump} = Roundup\left(\frac{W_{pump}}{W_{pump,max}}\right) \quad (3.3.16)$$

Where  $W_{pump,max}$  is the maximum capacity of a pump unit. The total investment cost for the compressor and pump,  $C_{total}$ , in €, is given by the following equation:

$$C_{total} = C_{comp} * 10^6 + C_{pump} * 10^3 \quad (3.3.17)$$

The LCO2T for the initial compressor and pump investment,  $LCO2T_{comp/pump,Invest}$  can be calculated as:

$$LCO2T_{comp/pump,Invest} = \frac{C_{total} * CRF_{comp/pump}}{CF_{comp/pump} * m_{CO2,year}} \quad (3.3.18)$$

Where  $CRF_{comp/pump}$  is the capital recovery factor for compressors and pumps and  $CF_{comp/pump}$  is the capacity factor of the compressor and pump.

The annual operation and maintenance cost of compressors and pumps,  $O\&M_{annual}$  is considered to be 4% of the total investment cost and is given by:

$$O\&M_{annual} = C_{total} * 0.04 \quad (3.3.19)$$

The annual energy cost for compression and pumping,  $E_{annual}$ , is calculated as:

$$E_{annual} = p_e * (W_{comp} + W_{pump}) * 365 * 24 \quad (3.3.20)$$

Where  $p_e$  is the electricity cost in €/KWh, with  $W_{comp}$  and  $W_{pump}$  in KW.

Finally, the LCO2T for initial compressor and pump energy costs,  $LCO2T_{comp/pump,Energy}$  is computed as:

$$LCO2_{comp/pump,Energy} = \frac{E_{annual}}{m_{CO2,year}} \quad (3.3.21)$$

## 4 Case Study

### 4.1 Executive Summary

This case study is based on the analysis and sizing of all the infrastructure necessary for the conditioning of CO<sub>2</sub> captured from the emissions coming from an energy recovery facility in Custóias (Porto) from which waste incineration takes place and further transport to the Porto de Leixões seaport.

Pre-treated flue gas is transported to the CO<sub>2</sub> capture facilities on the site via duct pipeline. CO<sub>2</sub> is captured and continually transported by duct pipes to the seaport.

At the seaport the CO<sub>2</sub> is liquefied for being stored temporarily, before being offloaded to CO<sub>2</sub> carriers for transport to the storage operator.

This infrastructure should be capable of transporting 400 000 tCO<sub>2</sub>/yr resulting from the incineration of waste material.

### 4.2 Problem Set up and Assumptions

The total emissions from the waste incineration plant are expected to be on the order of 400 000 tCO<sub>2</sub>/yr.

The pipeline starts on the incineration plant on Custóias and terminates on Porto de Leixões.

The pipeline outline is represented on figure 23 in a mere indicative route for initial assessment purposes.

This project is based on the following assumptions:

- Theoretically, the pressure might decrease to 80 bar before requiring a booster pump because the cutoff pressure for CO<sub>2</sub> phase shift at 30°C is 73.8 bar. However, a more careful approach is taken due to the substantial expenses associated with transitioning CO<sub>2</sub> from gas to the dense phase. Consequently, 100 bar is established as the lowest permitted pressure, [15]
- The pipeline is to be buried at a depth of one metre, with ambient temperature remaining constant. It is assumed that there is no heat exchange in the pipeline, [13].
- Pressure losses due to friction are considered dominant compared to losses due to bends, [13].
- Amount of impurities in the stream are assumed to be negligible and without effect on the flow characteristics of CO<sub>2</sub> gas, [13].
- The detailed topographical model of the region is unknown following that the landscape is taken to be level. As a result, the pipeline profile is assumed to be level with no height variations, [13].

- Selected pipe class is seamless. Seam joint factor (E) is therefore 1.0, [13]
- Pipe material is assumed to be steel (DIN 2448)
- The roughness for the pipeline is the common used for steel pipes,  $\varepsilon$ , is  $4.5E-05$  m, [15].
- In terms of temperature drop, it is assumed that the  $CO_2$  inlet temperature, flow rate, and burial depth have the largest effects on temperature drop, when comparing to the ground temperature, indicating that there is no need for applying an insulation layer to the pipeline, [16].

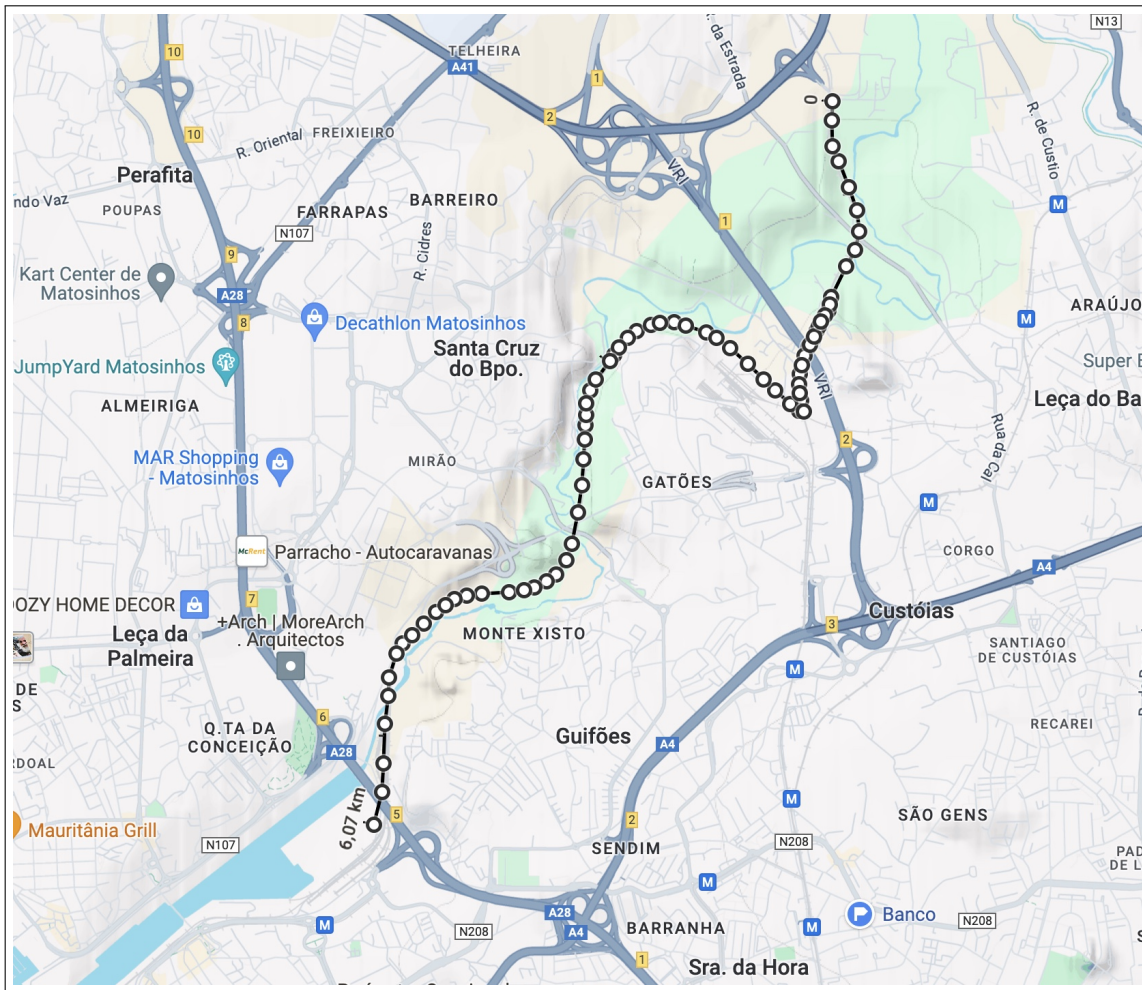


Figure 23: Pipeline Outline.

### 4.3 Results And Discussion

The simulation for the current case study was performed on Aspen Plus. The method choosen for simulating carbon dioxide properties was the Refrigerant Property method (REFPROP).

Figure 24 that follows represents the flowsheet that was created for the simulation. The treated fluegas from the incineration plant (COMPIN) enters a multistage compression system (CO2COMP), where it is compressed with 5 stages from an initial pressure of 1 bar to an outlet pressure of 73,8 bar, [15].

The compressed CO2 (COMPOUT) is then pumped (PUMP) until reaching a pressure which allows for a pressure at the pipeline outlet of 100 bar. The pumped CO2 (PUMPOUT) then enters the pipeline where it suffers a pressure drop until the pipeline outlet. The CO2 at the end of the pipeline was denoted as PIPEOUT.

For the multi stage compression system (CO2COMP), it was considered a fixed discharge pressure of 73,8 bar and an isentropic efficiency of 0,8 on each compression stage. It was also considered that the compressor was cooled at each compression stage with an outlet temperature for the coolant of 30 °C, [15].

For the pump, the efficiency was set to 0,75, [15], and the discharge pressure was fixed to 105,85 bar. This value for the discharge pressure was attained from the pressure drop along the pipeline (5,85 bar), where it was added 100 bar which corresponds to the minimum value for the pressure at the pipeline outlet.

The value for the pipe diameter was obtained from the economical analysis presented on section 4.3.1 were it was concluded that the most cost-beneficial value for the diameter was to use a normalized diameter, DN, of 125 mm. This gives an outter diameter of 139,7 mm with a wall thickness of 4 mm, and an internal diameter, D, of 131,7 mm considering the norm DIN 2448 (see ANNEX B).

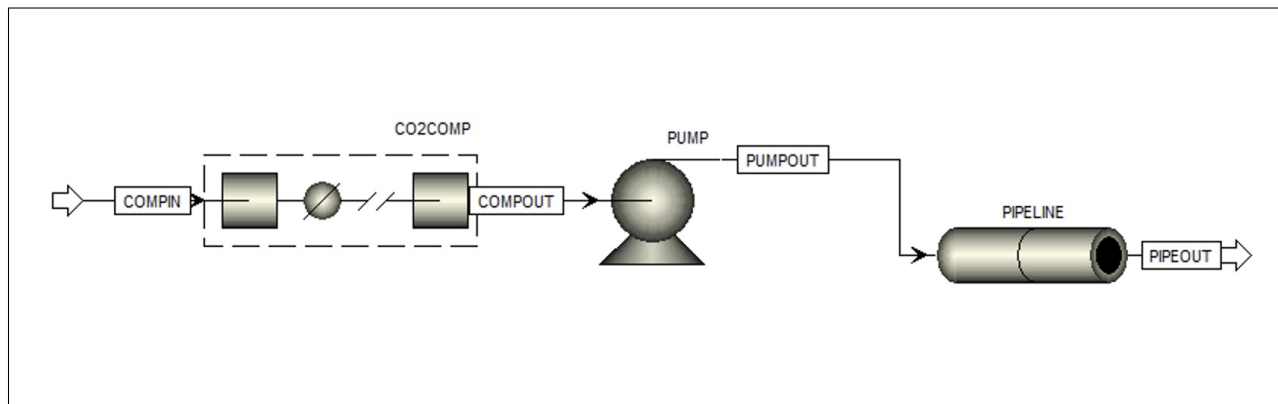


**Figure 24:** Flowsheet used on Aspen Plus.

The following table 4 presents a summary of all the assumptions used for the simulation:

**Table 4:** Assumptions used for the simulation.

	Parameter	Value	Unit
<b>Material line</b>			
COMPIN	Temperature [15]	30	°C
	Pressure [15]	1	bar
	Mass flow rate	400 000 tons/year	
	Volume flow rate	23596.5	m <sup>3</sup> /h
<b>Equipment</b>			
CO2COMP	Number of stages [15]	5	
	Discharge pressure [15]	73.8	bar
	Isentropic efficiency [15]	0,8	
	Coolant outlet temperature	30	°C
Pump	Efficiency [15]	0.75	
	Discharge pressure [15]	105.85	bar
Pipeline	Pipe length	6000	m
	Inner diameter	0.125	m
	Roughness [15]	0.045	mm

The results obtained for each of the 5 compression stages in the multi stage compressor (CO2COMP) are presented on figure 25:

Stage	Temperature	Pressure	Pressure ratio	Indicated power	Brake horsepower	Head developed	Volumetric flow	Efficiency used
	C	bar		kW	kW	meter	cum/hr	
▶ 1	106,493	2,3638	2,3638	774,878	774,878	5497,32	23596,5	0,8
▶ 2	106,625	5,58756	2,3638	769,611	769,611	5459,95	9917,5	0,8
▶ 3	106,927	13,2079	2,3638	757,038	757,038	5370,75	4129,64	0,8
▶ 4	107,573	31,2209	2,3638	726,554	726,554	5154,49	1678,55	0,8
▶ 5	108,338	73,8	2,3638	648,907	648,907	4603,63	633,777	0,8

**Figure 25:** Multi stage compressor profile results.

Adding all contributions from each compression stage, we get a total compression power,  $W_{comp}$ , of 3678 KW.

Regarding the cooling load necessary for each compression stage (considering a coolant outlet temperature of 30 °C at each compression stage), it was attained the results on figure 26:

Stage	Temperature C	Pressure bar	Duty kW	Vapor fraction
▶ 1	30	2,3638	-789,015	1
▶ 2	30	5,58756	-803,667	1
▶ 3	30	13,2079	-841,478	1
▶ 4	30	31,2209	-955,084	1
▶ 5	30	73,8	-2762,87	0

Figure 26: Multi stage compressor inter stage cooling results.

From figure 26 we can conclude that the total cooling power needed is 6152.11 KW.

Finally considering the simulation results obtained for the pump, they are presented on figures 27 and 28:

Fluid power	57,2130082	kW
Brake power	76,284	kW
Electricity	76,284	kW
Volumetric flow rate	64,2642	cum/hr
Pressure change	32,05	bar
NPSH available	28,6982	meter
NPSH required		
Head developed	507,367	meter
Pump efficiency used	0,75	
Net work required	76,284	kW
Outlet pressure	105,85	bar
Outlet temperature	38,9812	C

Figure 27: Summary of the simulation results attained for the pump part A.

	▼
User tag number	PUMP
Remarks 1	Equipment mapped from 'PUMP'.
Quoted cost per item [USD]	
Currency unit for matl cost	
Number of identical items	
Installation option	
Casing material	
Liquid flow rate [l/min]	1178,17
Fluid head [meter]	508,155
Speed [rpm]	
Fluid specific gravity	0,644057
Driver power [kW]	
Driver type	
Seal type	
Design gauge pressure [barg]	110,129
Design temperature [C]	121,111
Fluid viscosity [cP]	0,5
Pump efficiency [fraction]	0,75
Allow resize	

Figure 28: Summary of the simulation results attained for the pump part B.

Table 5 that follows depicts the  $CO_2$  stream properties at each step of the simulation:

Table 5: Assumptions used for the simulation.

Material line	Parameter	Value	Unit
COMPOUT	Temperature	30	°C
	Pressure	73.8	bar
	Volume flow rate	64.26	$m^3/h$
PUMPOUT	Temperature	39	°C
	Pressure	105.85	bar
	Volume flow rate	60.86	$m^3/h$
PIPEOUT	Temperature	37.77	°C
	Pressure	99.99	bar
	Volume flow rate	61.71	$m^3/h$

### 4.3.1 Cost Analysis Results

The following section presents a detailed cost analysis for the pipeline as well as both the compressor and pump infrastructure considering the initial investment and operations and maintenance, O&M, costs.

#### Pipeline

The pipeline's associated costs can be separated into two categories: investment costs and operating costs. For the computation of the different cost variables, it was performed the following assumptions:

**Table 6:** Pipeline-related assumptions.

<b>Assumption</b>	<b>Value</b>	<b>Unit</b>
Pipeline Normalized Diameter (DN)	125	mm
Capacity factor ( $CF_{pipe}$ ) [15]	90%	
Interest rate (i) [15]	8%	
Lifetime (n) [15]	50	years
Fix O&M factor [15]	2.6%	
Cumulative inflation rate of € from 2010 to 2024 ( $I_{cum}$ ) [15]	36,55%	
Annual $CO_2$ mass flow-rate ( $m_{CO_2,year}$ )	400 000	t/year

The following table 7 shows the results obtained for all the variables associated to the pipeline costs:

**Table 7:** Pipeline-related cost results.

Variable	Value	Unit
Investment cost of the pipeline ( $IC_{pipe}$ )	283.21	€/m
Total investment cost of the pipeline ( $Invest_{pipe}$ )	1699241	€
Pipeline's operation and maintenance expenses ( $O\&M_{pipe}$ )	44180	€/year
Capital recovery factor of the pipeline ( $CRF_{pipe}$ )	0,082	
Levelized cost of carbon dioxide transport for pipeline investment ( $LCO2T_{pipe,Invest}$ )	0.386	€/t
Levelized cost of carbon dioxide transport for pipeline O&M costs ( $LCO2T_{pipe,O\&M}$ )	0.123	€/t
Total ( $LCO2T_{pipe}$ )	0.509	€/t

### Compressor and Pump

For the discrimination of the different costs associated to both the compressor and the pump, the equations previously presented on section 3.3 were used considering the assumptions used by Soloman et al. (reference [15]), with the proper adaptations to this case study. The following tables 8 to 10 represent all the different assumptions used for the calculations.

**Table 8:** Compressor and pump-related assumptions.

Assumption	Value	Unit
Interest rate (i) [15]	8%	
Lifespan (n) [15]	15	years
Capacity factor ( $CF_{comp/pump}$ ) [15]	90%	
Electricity price ( $p_e$ )	0.15	€/KWh
Multiplication exponent (me) [15]	0.9	
Cumulative inflation rate of € from 2010 to 2024 ( $I_{cum}$ ) [15]	36.55%	
Universal gas constant (R) [15]	8.314	KJ/(KmolK)
Molecular weight of CO2 (M) [15]	44.01	Kg/kmol

**Table 9:** Compressor -related assumptions.

<b>Assumption</b>	<b>Value</b>	<b>Unit</b>
<b>Compressor</b>		
Inlet temperature ( $T_{in,comp}$ ) [15]	313.15	K
Inlet pressure ( $P_{initial}$ ) [15]	1	bar
Outlet pressure ( $P_{cut-off}$ ) [15]	73.8	bar
Number of compression stages ( $N_{stage}$ ) [15]	5	
Compressor isentropic efficiency ( $\eta_{is}$ ) [15]	80%	
Compressor base cost ( $C_{0,comp}$ ) [15]	21.9	M€
Compressor base scale ( $W_0$ ) [15]	13 000	KW
Compressor scaling factor ( $y_{comp}$ ) [15]	0.67	
Maximum compressor capacity ( $W_{comp,max}$ ) [15]	35 000	KW

**Table 10:** Pump-related assumptions.

<b>Assumption</b>	<b>Value</b>	<b>Unit</b>
<b>Pump</b>		
Inlet temperature ( $T_{in,pump}$ ) [15]	303.15	K
Inlet pressure ( $P_{cut-off}$ ) [15]	73.8	bar
Outlet pressure ( $P_{final}$ )	105.85	bar
Pumping efficiency ( $\eta_p$ ) [15]	75%	
Pump base cost ( $C_{0,pump}$ ) [15]	74.3	K€
Pump scaling factor ( $y_{pump}$ ) [15]	0.58	
Maximum pump capacity ( $W_{pump,max}$ ) [15]	2000	KW

The following table 11 presents all the results obtained for the calculations associated to the compressor and the pump:

**Table 11:** Compressor and pump-related cost results.

Variable	Value	Unit
Compressor investment cost ( $C_{comp}$ )	12.89	M€
Pump investment cost ( $C_{pump}$ )	1253.37	k€
Total investment of compressor and pump ( $C_{total}$ )	14143331	€
Capital recovery factor for compressor and pump ( $CRF_{comp/pump}$ )	0.12	
Levelized cost of initial compressor and pump investment ( $LCO2T_{comp/pump,Invest}$ )	4.59	€/t
Annual operations and maintenance costs for compressor and pump ( $O\&M_{annual}$ )	565733	€/year
Levelized cost of compressor and pump O&M ( $LCO2T_{comp/pump,O\&M}$ )	1.57	€/t
Annual energy cost of compression and pumping ( $E_{annual}$ )	4964752	€/year
Levelized cost of compressor and pump energy ( $LCO2T_{comp/pump,Energy}$ )	12.41	€/t

Figure 29 shows a comparison for the levelized cost of CO<sub>2</sub> transport (LCO<sub>2</sub>T) considering pipe sizes of 90, 100, 125 and 150 mm. Pipe (Invest + O&M) is the total levelized cost of the pipeline considering both investment and operation/maintenance; Comp/pump (Invest + O&M) is the total levelized cost of the compressor and the pump considering both investment and operation/maintenance and Comp/pump (Energy) is the levelized cost associated to the energy necessary for compressing and pumping the CO<sub>2</sub>.

Analysing figure 29 it is clear to see that the most cost-beneficial pipe diameter is 125 mm which is associated to the lowest total levelized cost (19,05 €/t).

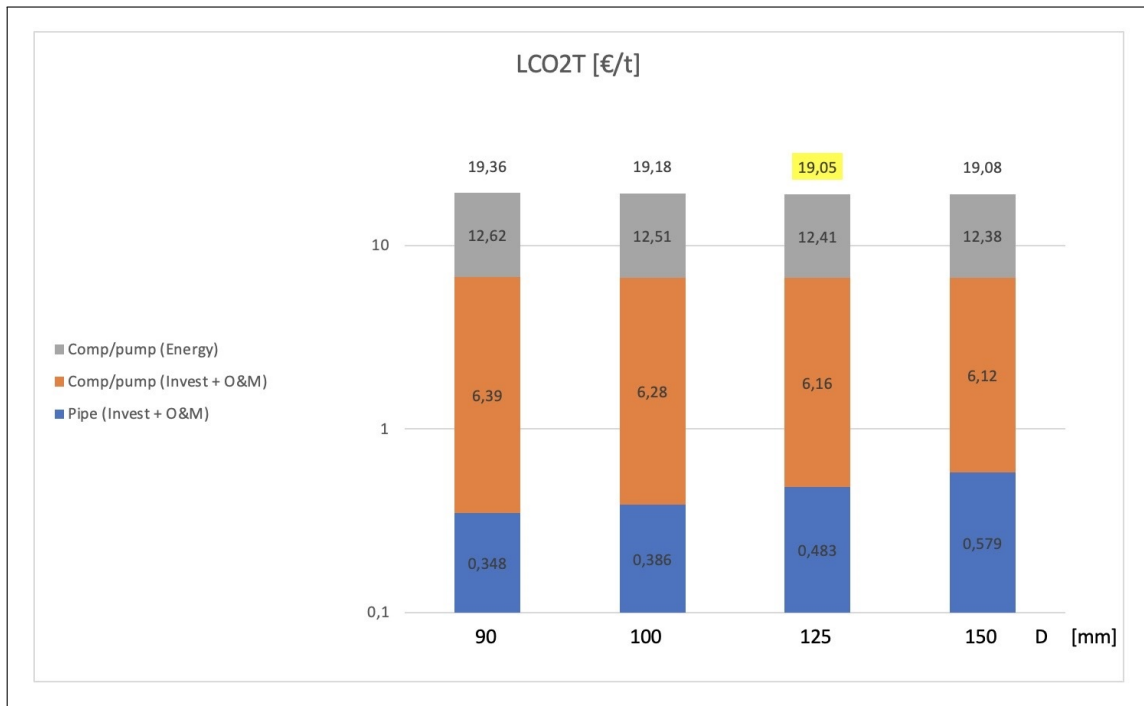


Figure 29: Levelized cost of carbon dioxide transport for different pipe diameters.

### Sensitivity Analysis

Figure 30 depicts the results of a sensitivity analysis conducted to assess the influence of specific parameters on CO2 transportation costs. The analysis varied factors such as interest rates, pipeline lifetime, pipeline O&M factor and pipeline investment cost by +/- 20 % to evaluate their impact on the total LCO2T. This sensitivity analysis was conducted for the assumptions of this case study, i.e. transportation of 400 000 t/year of CO2 over a distance of 6 Km, considering a pipe size of 125 mm.

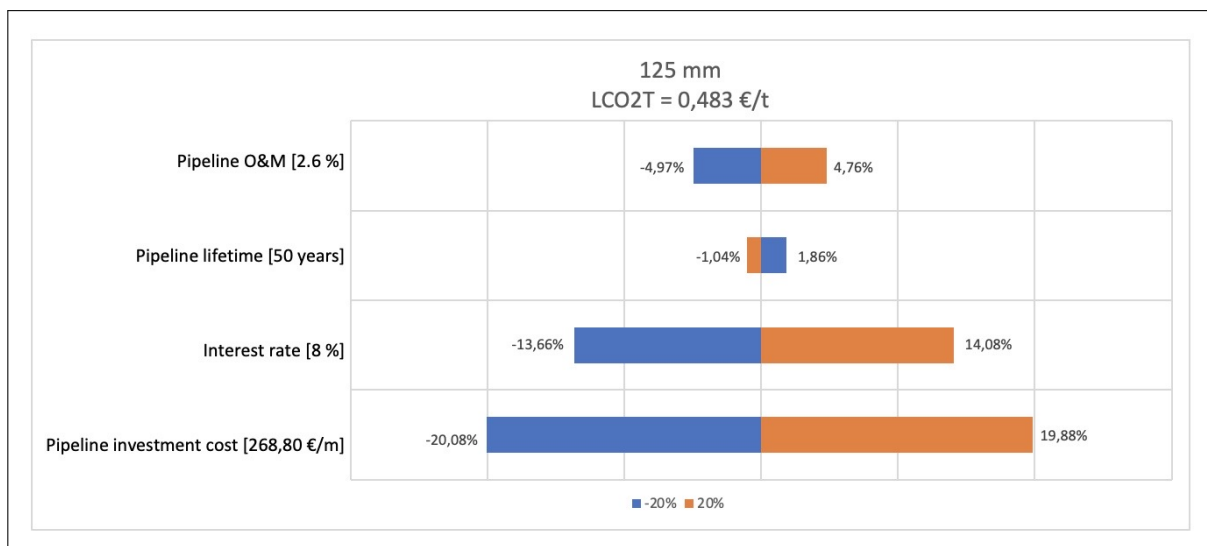


Figure 30: Sensitivity analysis for pipe DN 125 mm.

According to the sensitivity analysis, pipeline investment has the biggest impact on the overall LCO<sub>2</sub>T. The main source of the overall LCO<sub>2</sub>T in the scenario taken into consideration for this case study is pipeline investment. The investment also takes O&M expenses into account. Furthermore, the interest rate has a major effect on the overall LCO<sub>2</sub>T. Therefore, the project's size and investment are crucial factors in figuring out the total LCO<sub>2</sub>T. In comparison, factors like pipeline longevity and O&M have less of an impact.

Figure 30 shows a comparison for the least levelized transport cost of CO<sub>2</sub> including the initial compression costs considering a CO<sub>2</sub> pressure increase up to 150 bar. In this comparison it was considered four different amounts of CO<sub>2</sub> to be transported: 200 000, 400 000, 600 000 and 800 000 tCO<sub>2</sub>/year along various distances up to 100 km for four different pipe sizes: 100, 125, 150 and 200 mm.

As it is expected the LCO<sub>2</sub>T increases with the increase in pipeline length and suffers an abrupt increase whenever the addition of a booster station becomes necessary, i.e. when the pressure drop becomes greater than 50 bar.

Analysing figure 31 it can be seen that for a flow rate of 200 000 tCO<sub>2</sub>/year it is more cost beneficial to use a pipe size of 100 mm for distances up to 70 km from which it becomes necessary to add a booster station and the pipe size of 125 mm becomes the most cost beneficial option.

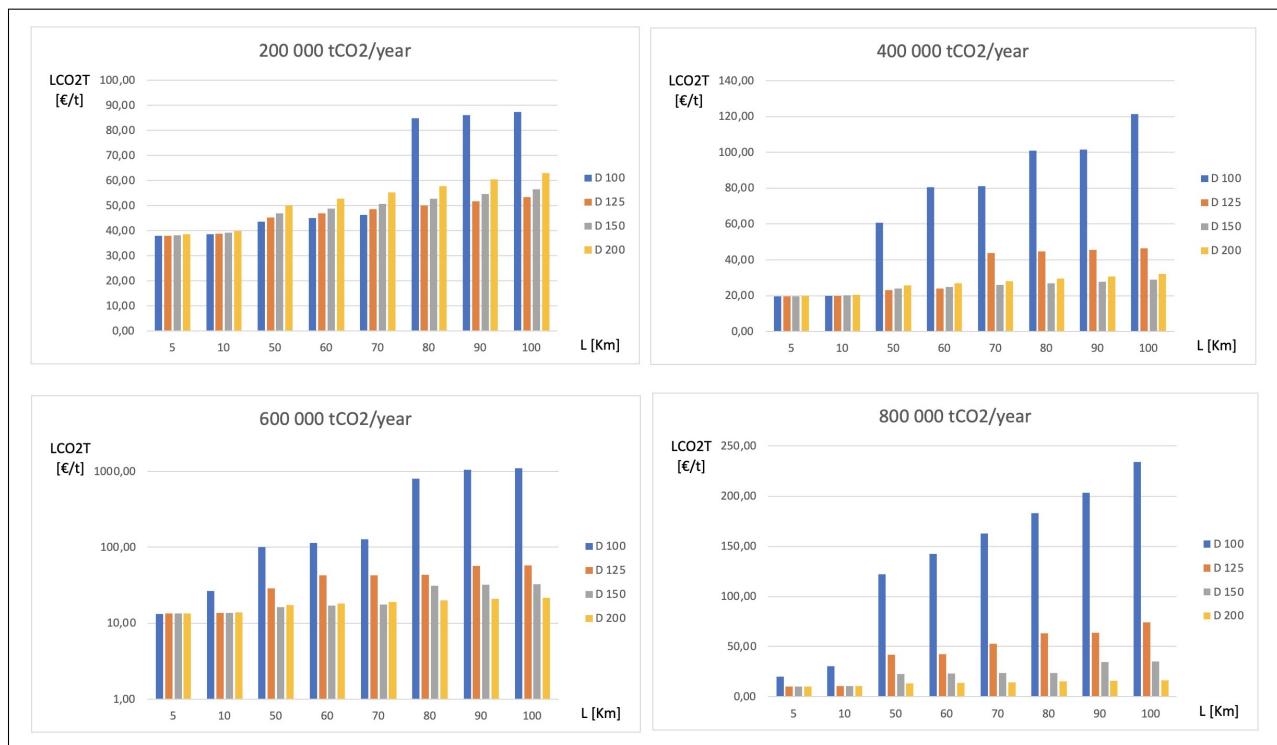


**Figure 31:** Least Levelized transport cost of CO<sub>2</sub> including initial compression for different mass flow rates.

The complete information for the values of the LCO<sub>2</sub>T can be found on figure 32

D 100 mm									
	LCO2T (€/t)	Distance (Km)							
		5	10	50	60	70	80	90	100
Mass flow (t/year)	200 000	37,84	38,48	43,63	44,92	46,21	84,69	85,97	87,26
	400 000	19,46	19,78	60,62	80,4	81,05	100,83	101,47	121,25
	600 000	13,29	26,59	99,80	113,35	126,90	805,34	1052,78	1093,18
	800 000	20,23	30,43	122,04	142,44	162,83	183,22	203,62	234,05

D 125 mm									
	LCO2T (€/t)	Distance (Km)							
		5	10	50	60	70	80	90	100
Mass flow (t/year)	200 000	38,00	38,80	45,24	46,85	48,46	50,07	51,68	53,28
	400 000	19,54	19,94	23,16	23,96	43,90	44,71	45,51	46,32
	600 000	13,35	13,62	28,84	42,46	42,99	43,53	57,14	57,68
	800 000	10,24	10,44	42,16	42,56	53,00	63,43	63,84	74,27

D 150 mm									
	LCO2T (€/t)	Distance (Km)							
		5	10	50	60	70	80	90	100
Mass flow (t/year)	200 000	38,16	39,13	46,85	48,78	50,71	52,64	54,57	56,50
	400 000	19,62	20,10	23,96	24,93	25,89	26,86	27,82	28,79
	600 000	13,40	13,72	16,30	16,94	17,58	31,31	31,95	32,59
	800 000	10,28	10,52	22,49	22,97	23,45	23,93	34,45	34,93

D 200 mm									
	LCO2T (€/t)	Distance (Km)							
		5	10	50	60	70	80	90	100
Mass flow (t/year)	200 000	38,48	39,77	50,07	52,64	55,22	57,79	60,36	62,94
	400 000	19,78	20,42	25,57	26,86	28,15	29,43	30,72	32,01
	600 000	13,51	13,94	17,37	18,23	19,09	19,94	20,8	21,66
	800 000	10,36	10,68	13,25	13,9	14,54	15,18	15,83	16,47

**Figure 32:** Least Levelized transport cost of CO<sub>2</sub> including initial compression for different mass flow rate and distances considering pipe sizes of 100, 125, 150 and 200 mm.

Finally, figure 33 depicts the maximum distance (in Km) for the pipeline without the necessity of using a booster station, for different CO<sub>2</sub> mass flows and pipe sizes of 100, 125, 150 and 200 mm considering an initial CO<sub>2</sub> compression to 150 bar.

Maximum distance without a booster station (km)					
Max Distance [km]		D [mm]			
		100	125	150	200
Mass flow (t/year)	200 000	75	203	523	2300
	400 000	19	60	132	590
	600 000	8	27	70	264
	800 000	4,5	15	40	149

**Figure 33:** Maximum safety distance for CO<sub>2</sub> pipeline transportation without a booster station.

This table shows that even if we doubled the CO<sub>2</sub> mass flow rate considered for this case study to 800 000 tCO<sub>2</sub>/year, we would still be capable of safely transporting CO<sub>2</sub> up to a distance of 15 km without any booster station.

## 5 Conclusion

The observed consequences of climate change call for and urgent development an more intensive use of carbon capture technologies.

The study performed on this dissertation comprised the analysis of different key-aspects that directly impact the cost of  $CO_2$  pipeline transport such as pipe diameter, pipe length, and flow rate.

A critical aspect that drastically impacts the transport costs is whenever the addition of booster stations becomes necessary. Whenever this happens it may become economically more advantageous to increase the pipe size.

It was concluded that for an annual transport of 400 000 t $CO_2$ /year through a 6 km pipeline the most cost beneficial pipe size to be used is 125 mm. This pipe size results on a total Least Levelized Transport Cost (LCO2T) including initial compression of  $CO_2$  of 19.05 €/t.

The economical analysis performed on  $CO_2$  pipeline transport considering flow rates that ranged from 200 000 to 800 000 t/year and pipeline length from 5 to 100 km with pipe sizes of 100, 125, 150 and 200 mm led to the following conclusions:

- The total Least Levelized Transport cost for  $CO_2$  including initial compression (LCO2T) presented a minimum value of 10.24 €/t in the case of transporting 800 000 t $CO_2$ /year along 5 km with a pipe size of 125 mm.
- Inadequate pipe sizing can result on drastic increases in transport costs directly caused by the necessity to implement more booster stations along the pipeline.
- The maximum distance that can be used for the pipeline without the need of any booster station is another key aspect to be taken into account where for the range of flow rate and pipe size considered in this study, this maximum distance ranged from 4.5 km all the way to 2300 km.

In summary, a variety of variables, such as transport mass, distance, and the number of booster stations, affect the ideal pipeline diameter for transporting  $CO_2$ . To choose the best mode of transportation, special attention should also be paid to pipeline investment, operating costs, energy costs, and interest rates. This all-encompassing strategy guarantees successful and economical planning of  $CO_2$  transportation infrastructure.

Future research may emphatize the following aspects:

- Perform an economical analysis along a wider range of either distances and  $CO_2$  flow rates.
- Analyse the viability of utilizing the existing natural gas pipeline infrastructure for transporting  $CO_2$  at a phase that may be compatible to this type of transport and perform an economical cost comparison.
- Study the costs that would result if the transport was performed by other  $CO_2$  transport methods such as by truck or by trail.

## 6 References

[1] IPCC, 2014: Climate Change 2014: Synthesis Report. Contribution of Working Groups I, II and III to the Fifth Assessment Report of the Intergovernmental Panel on Climate Change [Core Writing Team, R.K. Pachauri and L.A. Meyer (eds.)]. IPCC, Geneva, Switzerland, 151 pp;

[2] Global CCS Institute, 2020: GLOBAL STATUS OF CCS. Contribution of the team led by: Brad Page, Guloren Turan and Alex Zapantis

[3] International Energy Agency. (2020). Energy Technology Perspectives 2020, Special Report on Carbon Capture Utilisation and Storage. <https://webstore.iea.org/download/direct/4191>

[4] Global CCS Institute, 2012: CO2 CAPTURE TECHNOLOGIES, PRE COMBUSTION CAPTURE.

[5] Chapter 11 - Gaseous Emissions and the Environment, Editor(s): Claire Soares, Gas Turbines (Second Edition), Butterworth-Heinemann, 2015, Pages 637-667, ISBN 9780124104617

(<https://doi.org/10.1016/B978-0-12-410461-7.00011-0>)

[6] Allen, M.R., O.P. Dube, W. Solecki, F. Aragón-Durand, W. Cramer, S. Humphreys, M. Kainuma, J. Kala, N. Mahowald, Y. Mulugetta, R. Perez, M. Wairiu, and K. Zickfeld, 2018: Framing and Context. In: Global Warming of 1.5°C. An IPCC Special Report on the impacts of global warming of 1.5°C above pre-industrial levels and related global greenhouse gas emission pathways, in the context of strengthening the global response to the threat of climate change, sustainable development, and efforts to eradicate poverty [Masson-Delmotte, V., P. Zhai, H.-O. Pörtner, D. Roberts, J. Skea, P.R. Shukla, A. Pirani, W. Moufouma-Okia, C. Péan, R. Pidcock, S. Connors, J.B.R. Matthews, Y. Chen, X. Zhou, M.I. Gomis, E. Lonnoy, T. Maycock, M. Tignor, and T. Waterfield (eds.)]. Cambridge University Press, Cambridge, UK and New York, NY, USA, pp. 49-92, doi:10.1017/9781009157940.003.

[7] IEA (2023), World Energy Outlook 2023, IEA, Paris <https://www.iea.org/reports/world-energy-outlook-2023>, Licence: CC BY 4.0 (report); CC BY NC SA 4.0 (Annex A)

[8] IEA (2023), CO2 Emissions in 2022, IEA, Paris <https://www.iea.org/reports/co2-emissions-in-2022>, Licence: CC BY 4.0

[9] Carbon Dioxide Capture Handbook, U.S Department of Energy (DOE) and National Energy Technology Laboratory (NETL), United States, 2015. Accessed: Apr. 2024. [online]. Available: <https://netl.doe.gov/sites/default/files/netl-file/Carbon-Dioxide-Capture-Handbook-2015.pdf>

[10] Global CCS Institute, 2021: Technology Readiness and Costs of CCS.

[11] Witkowski, Andrzej; Majkut, Mirosław; and Rulik, Sebastian. (2014). Analysis of pipeline transportation systems for carbon dioxide sequestration. Archives of Thermodynamics. 35. s. 117-140. 10.2478/aoter-2014-0008.

[12] McKaskle, Ray and Beitler, Carrie and Dombrowski, Katherine and Fisher, Kevin, The Engineer's Guide to CO2 Transportation Options (October 23, 2022). Proceedings of the 16th

Greenhouse Gas Control Technologies Conference (GHGT-16) 23-24 Oct 2022, Available at SSRN: <https://ssrn.com/abstract=4278858> or <http://dx.doi.org/10.2139/ssrn.4278858>

[13] Lazic, Tihomir and Oko, Eni and Wang, Meihong. (2013). Case study on CO<sub>2</sub> transport pipeline network design for Humber region in the UK. Proceedings of the Institution of Mechanical Engineers Part E Journal of Process Mechanical Engineering. 228. 10.1177/0954408913500447.

[14] Munish Kumar Chandel, Lincoln F. Pratson, Eric Williams, Potential economies of scale in CO<sub>2</sub> transport through use of a trunk pipeline, Energy Conversion and Management, Volume 51, Issue 12, 2010, Pages 2825-2834, ISSN 0196-8904 <https://doi.org/10.1016/j.enconman.2010.06.020>.

[15] Solomon, Mithran & Scheffler, Marcel & Heineken, Wolfram & Ashkavand, Mostafa & Birth-Reichert, Torsten. (2024). Pipeline Infrastructure for CO<sub>2</sub> Transport: Cost Analysis and Design Optimization. Energies. 17. 2911. 10.3390/en17122911.

[16] B. Wetenhall, J.M. Race, H. Aghajani, J. Barnett, The main factors affecting heat transfer along dense phase CO<sub>2</sub> pipelines, International Journal of Greenhouse Gas Control, Volume 63, 2017, Pages 86-94, ISSN 1750-5836, <https://doi.org/10.1016/j.ijggc.2017.05.003>. (<https://www.sciencedirect.com/s>

# Appendices

## A Annex Physical properties of carbon dioxide

### Phase Diagram

The phase diagram of carbon dioxide (CO<sub>2</sub>) illustrates the different phases (solid, liquid, and gas) of CO<sub>2</sub> under varying temperatures and pressures (see Figure A.1).

An uncommon characteristic of CO<sub>2</sub> is the existence of a triple point where all three phases (solid, liquid and gas) coexist in equilibrium. It is a point at a specific pressure and temperature where CO<sub>2</sub> can exist simultaneously as solid, liquid and gas.

Other key feature for carbon dioxide is it's critical point that occurs at a temperature of 31,04 °C and at a pressure of 7,39 MPa. For values of temperature and pressure above the critical ones, distinct liquid and gas phases no longer exist, and we enter the supercritical region.

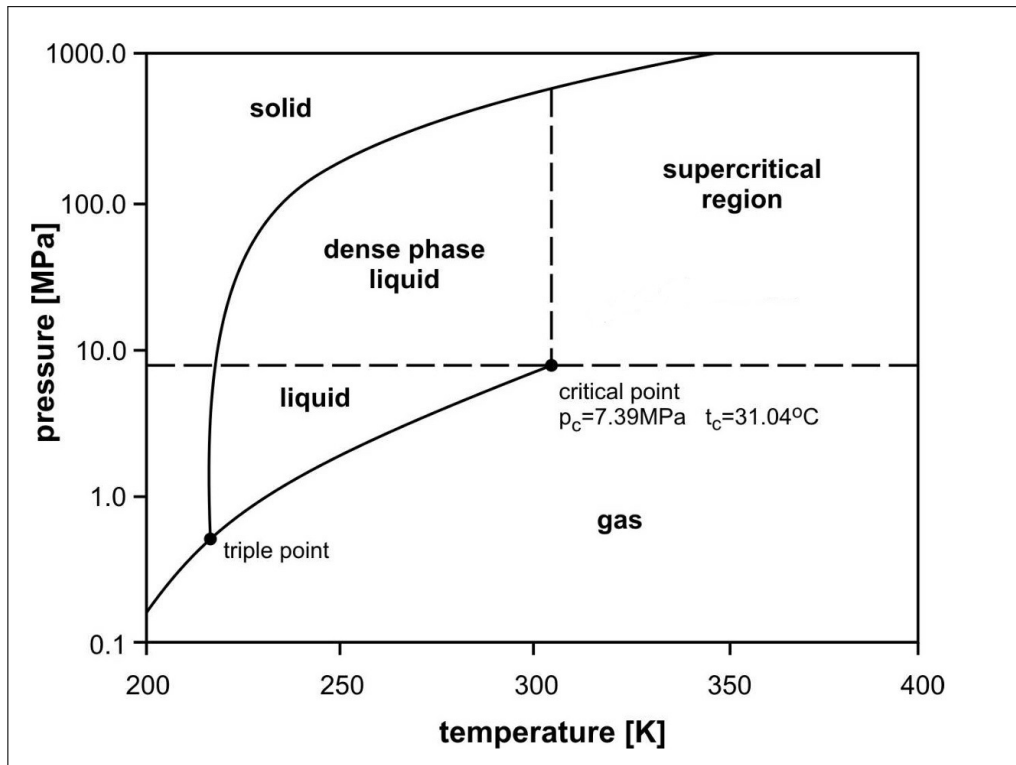


Figure A.1: A phase diagram for CO<sub>2</sub>., adapted from [11].

### Compressibility

One key aspect to have into consideration when developing technologies for carbon storage and specially regarding carbon transport is the compressibility of CO<sub>2</sub>.

Figure A.2 shows the variation that CO<sub>2</sub> compressibility has with pressure for different values of

temperature and impurities. As it is clear to see, carbon dioxide compressibility varies nonlinearly with pressure and changes drastically for ranges of pressure lower than 8.6 MPa (approximately) [11].

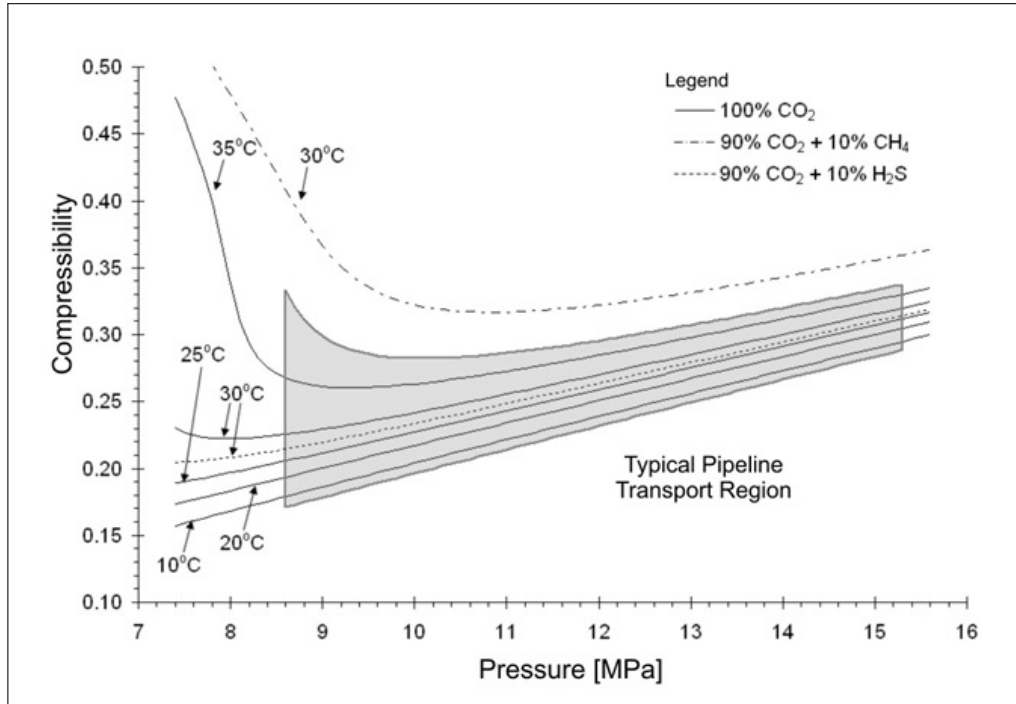


**Figure A.2:** Nonlinear compressibility of CO<sub>2</sub> in the range of pressures common for pipeline transport as predicted by the Peng-Robinson equation of state, [11].

## B Pipe size of seamless steel pipe DIN 2448

This annex shows the different values for the pipe sizes associated to the norm DIN 2448. Figure 25 shows all the standard diameter sizes associated to this norm DIN.

DIAMETRO NOMINAL		DIMENSÕES		PESO Negro Kg/m	PESO Pintado Kg/m	DIAMETRO NOMINAL		DIMENSÕES		PESO Negro Kg/m	PESO Pintado Kg/m
DN	In.	D mm	e mm			DN	In.	D mm	e mm		
6	1/8"	10,2	1,6	0,34	0,35	150	6"	168,3	4,5	18,18	18,31
8	1/4"	13,5	1,8	0,52	0,53	175	7"	193,7	5,6	25,98	26,13
10	3/8"	17,2	1,8	0,68	0,7	200	8"	219,1	6,3	33,06	33,23
15	1/2"	21,3	2	0,95	0,97	225	9"	244,5	6,3	37,01	37,2
20	3/4"	26,9	2,3	1,4	1,42	250	10"	273	6,3	41,43	41,65
25	1"	33,7	2,6	1,99	2,02	300	12"	323,9	7,1	55,47	55,72
32	1 1/4"	42,4	2,6	2,55	2,59	350	14"	355,6	8	68,57	68,85
40	1 1/2"	48,3	2,6	2,93	2,97	400	16"	406,4	8,8	86,28	86,6
50	2"	60,3	2,9	4,1	4,15	450	18"	457	10	110,23	110,59
65	2 1/2"	76,1	2,9	5,23	5,29	500	20"	508	11	134,82	135,22
80	3"	88,9	3,2	6,76	6,83	550	22"	559	12,5	168,46	168,9
90	3 1/2"	101,6	3,6	8,7	8,78	600	24"	610	12,5	184,18	184,66
100	4"	114,3	3,6	9,83	9,92	650	26"	660	14,2	226,14	226,66
125	5"	139,7	4	13,39	13,5	700	28"	711	14,2	244	244,56

Figure B.1: Pipe size of seamless steel pipe DIN 2448.